2022

# Association among anterior maxillary dental arch form, alveolar bone thickness and sagittal root position of maxillary central incisor : a cone beam computed tomography analysis

Suttikiat Somvasoontra
*Faculty of Dentistry*

# ASSOCIATION AMONG ANTERIOR MAXILLARY DENTAL ARCH FORM, ALVEOLAR BONE THICKNESS AND SAGITTAL ROOT POSITION OF MAXILLARY CENTRAL INCISOR: A CONE BEAM COMPUTED TOMOGRAPHY ANALYSIS

Mr. Suttikiat Somvasoontra



A Thesis Submitted in Partial Fulfillment of the Requirements
for the Degree of Master of Science in Esthetic Restorative and Implant Dentistry
FACULTY OF DENTISTRY
Chulalongkorn University
Academic Year 2022

ความสัมพันธ์ระหว่างรูปแบบส่วนโค้งฟันหน้าขากรรไกรบนกับความหนาของกระดูกรอบรากฟันและแนวตำแหน่งแกนฟันในแนวดิ่งของฟันตัดบนซี่กลาง : วิเคราะห์โดยโคนบีมคอมพิวเตดโทโมกราฟฟี

นายสุทธิเกียรติ สมวสุนธรา



วิทยานิพนธ์นี้เป็นส่วนหนึ่งของการศึกษาตามหลักสูตรปริญญาวิทยาศาสตรมหาบัณฑิต
สาขาวิชาทันตกรรมบูรณะเพื่อความสวยงามและทันตกรรมรากเทียม ไม่สังกัดภาควิชา/เทียบเท่า
คณะทันตแพทยศาสตร์ จุฬาลงกรณ์มหาวิทยาลัย
ปีการศึกษา 2565

| | |
|---|---|
| Thesis Title | ASSOCIATION AMONG ANTERIOR MAXILLARY DENTAL ARCH FORM, ALVEOLAR BONE THICKNESS AND SAGITTAL ROOT POSITION OF MAXILLARY CENTRAL INCISOR: A CONE BEAM COMPUTED TOMOGRAPHY ANALYSIS |
| By | Mr. Suttikiat Somvasoontra |
| Field of Study | Esthetic Restorative and Implant Dentistry |
| Thesis Advisor | Associate Professor ATIPHAN PIMKHAOKHAM, D.D.S., M.P.A., Ph.D. |
| Thesis Co Advisor | Associate Professor PRAVEJ SERICHETAPHONGSE, D.D.S., M.S. |

Accepted by the FACULTY OF DENTISTRY, Chulalongkorn University in Partial Fulfillment of the Requirement for the Master of Science

..... Dean of the FACULTY OF DENTISTRY
(Professor Pornchai Jansisyanont, D.D.S., M.S., Ph.D.)

THESIS COMMITTEE

..... Chairman
(Professor MANSUANG ARKSORNNUKIT, D.D.S., M.S., Ph.D.)

..... Thesis Advisor
(Associate Professor ATIPHAN PIMKHAOKHAM, D.D.S., M.P.A., Ph.D.)

..... Thesis Co-Advisor
(Associate Professor PRAVEJ SERICHETAPHONGSE, D.D.S., M.S.)

..... Examiner
(D.D.S. Ph.D. WAREERATN CHENGPRAPAKORN)

..... External Examiner
(Assistant Professor Chanchai Wongchuensoontorn, D.D.S., M.D., Dr.med (Germany))

สุทธิเกียรติ สมวสุนธรา : ความสัมพันธ์ระหว่างรูปแบบส่วนโค้งฟันหน้าขากรรไกรบนกับความหนาของกระดูกรอบรากฟันและแนวตำแหน่งแกนฟันในแนวดิ่งของฟันตัดบนซี่กลาง : วิเคราะห์โดยโคนบีมคอมพิวเตดโทโมกราฟฟี. ( ASSOCIATION AMONG ANTERIOR MAXILLARY DENTAL ARCH FORM, ALVEOLAR BONE THICKNESS AND SAGITTAL ROOT POSITION OF MAXILLARY CENTRAL INCISOR: A CONE BEAM COMPUTED TOMOGRAPHY ANALYSIS) อ.ที่ปรึกษาหลัก : รศ. ทพ. ดร.อาทิพันธุ์ พิมพ์ขาวขำ, อ.ที่ปรึกษาร่วม : รศ. ทพ.ประเวศ เสรีเชษฐพงษ์

วัตถุประสงค์: เพื่อศึกษาความสัมพันธ์ระหว่างรูปแบบส่วนโค้งฟันหน้าขากรรไกรบน,อายุร่วมกับเพศและแนวตำแหน่งแกนฟันในแนวดิ่งเกี่ยวกับความหนาของกระดูกรอบรากฟันของฟันตัดบนซี่กลาง วิเคราะห์โดยโคนบีมคอมพิวเตดโทโมกราฟฟี

วิธีการศึกษา: คัดเลือก 280 ไฟล์ภาพรังสีส่วนตัดโคนบีมคอมพิวเตดโทโมกราฟฟีเพื่อนำมาจำแนกรูปแบบส่วนโค้งฟันหน้าขากรรไกรบนและจำแนกกลุ่มอายุร่วมกับเพศ จากนั้นนำ 560 ไฟล์ภาพรังสีส่วนตัดโคนบีมคอมพิวเตดโทโมกราฟฟีของฟันตัดบนซี่กลางมาวัดความหนาของกระดูกรอบรากฟันที่ระดับ 3 มิลลิเมตร จากรอยต่อเคลือบรากฟันกับเคลือบฟัน, กึ่งกลางราก และ ปลายราก ร่วมกับการจำแนกประเภทแนวตำแหน่งแกนฟันในแนวดิ่ง โดยใช้การวิเคราะห์ไคสแควร์, ทดสอบครัสคาล-วัลลิสและการวิเคราะห์การถดถอยเชิงเส้นพหุคูณ

ผลกรศึกษา: พบความแตกต่างอย่างมีนัยสำคัญของความหนากระดูกรอบรากฟันในแต่ละรูปแบบส่วนโค้งฟันหน้าขากรรไกรบนและแต่ละประเภทแนวตำแหน่งแกนฟันในแนวดิ่งที่บริเวณระดับปลายราก รูปแบบส่วนโค้งฟันรูปสี่เหลี่ยมและแนวตำแหน่งแกนฟันในแนวดิ่งประเภทที่ 1 แสดงความหนาของกระดูกมากที่สุดที่บริเวณระดับปลายรากในด้านเพดานปาก รูปแบบส่วนโค้งฟันรูปรีและแนวตำแหน่งแกนฟันในแนวดิ่งประเภทที่ 2 แสดงความหนาของกระดูกมากที่สุดที่บริเวณระดับปลายรากในด้านริมฝีปาก โดยไม่พบความสัมพันธ์ระหว่างรูปแบบส่วนโค้งฟันหน้าขากรรไกรบนกับประเภทแนวตำแหน่งแกนฟันในแนวดิ่ง และในกลุ่มผู้หญิงสูงอายุมีความสัมพันธ์กับการลดลงของความหนาของกระดูกรอบรากฟันอย่างมีนัยสำคัญและพบความสัมพันธ์เชิงลบในทุกตำแหน่ง

สรุปผลการทดลอง: รูปแบบส่วนโค้งฟันหน้าขากรรไกรบน,อายุร่วมกับเพศและแนวตำแหน่งแกนฟันในแนวดิ่งมีความสัมพันธ์ต่อกระดูกรอบรากฟันของฟันตัดบนซี่กลางในหลากหลายระดับ ดังนั้น ทันตแพทย์ควรนำปัจจัยทั้งหมดมาร่วมกันประเมินเพื่อประกอบการวางแผนในการทำทันตกรรมรากเทียม

| | | |
|---|---|---|
| สาขาวิชา | ทันตกรรมบูรณะเพื่อความสวยงามและทันตกรรมรากเทียม | ลายมือชื่อนิสิต ..... |
| ปีการศึกษา | 2565 | ลายมือชื่อ อ.ที่ปรึกษาหลัก ..... |
| | | ลายมือชื่อ อ.ที่ปรึกษาร่วม ..... |

# # 6175849732 : MAJOR ESTHETIC RESTORATIVE AND IMPLANT DENTISTRY
KEYWORD: Dental Arch, Alveolar process, Dental Implants, CBCT

Suttikiat Somvasoontra : ASSOCIATION AMONG ANTERIOR MAXILLARY DENTAL ARCH FORM, ALVEOLAR BONE THICKNESS AND SAGITTAL ROOT POSITION OF MAXILLARY CENTRAL INCISOR: A CONE BEAM COMPUTED TOMOGRAPHY ANALYSIS. Advisor: Assoc. Prof. ATIPHAN PIMKHAOKHAM, D.D.S., M.P.A., Ph.D. Co-advisor: Assoc. Prof. PRAVEJ SERICHETAPHONGSE, D.D.S., M.S.

Purpose: This study evaluated the association among the dental arch form, age-sex groups, and sagittal root position regarding alveolar bone thickness in the maxillary central incisor using cone-beam computed tomography (CBCT) images.

Materials and Methods: CBCT images of 280 patients were categorized based on the dental arch form and age-sex groups. Five hundred and sixty sagittal CBCT images of the maxillary central incisors were examined to measure the labial and palatal bone thickness at the root apex level, at the mid-root level and 3 mm apically from cemento-enamel junction, with SRP classification. Chi-square, Kruskal-Wallis test, and multiple linear regression were used for statistical analyses.

Results: Significant differences in alveolar bone thickness among the arch form and SRP. Square dental arch form and class I SRP showed the highest bone thickness at root apex levels of the palatal aspect. Taper dental arch form and class II SRP presented the highest bone thickness at the apex level of the labial aspect. No association between the distribution of dental arch form and SRP was found. The elderly female was significantly associated with thinner alveolar bone thickness and showed the negative correlation at all sites.

Conclusion: The patient's dental arch form, age-sex group, and sagittal root position affect their alveolar bone around maxillary central incisors in varying magnitude. Therefore, the clinician should take these combinations of factors into account when planning implant



| | | |
|---|---|---|
| Field of Study: | Esthetic Restorative and Implant Dentistry | Student's Signature ..... |
| Academic Year: | 2022 | Advisor's Signature ..... |
| | | Co-advisor's Signature ..... |

# ACKNOWLEDGEMENTS

First and foremost, I would like to express my sincere thanks to my advisor, Associate Professor Atiphan Pimkhaokham, and Associate Professor Pravej Serichetaphongsa, who has been immensely helpful and has provided me with essential consult guidance and encouragement. This research would not have been possible without their advice and assistance.

I would like to express my gratitude to Professor Mansuang Arksornnuki, Associate Professor Chanchai Wongchuensoontorn, and Asst. Prof. Dr.Wichit Tharanon, for sharing their knowledge and providing valuable suggestions that improved the research's approach.

I want to share my most profound appreciation for Asst. Prof. Dr.Soranun Chantarangsu for good recommendations and help regarding statistical approaches.

I am grateful to everyone at the ADTEC, National science park, Pathumthani, Mr.Teerapun Ponklang for CBCT technical support for the cone-beam computed tomography assistance, and Dr.Thanakorn Thimkam for improving the thesis's language.

Finally, I would like to express my heartfelt gratitude to my friends and my family for their love, kindness, and support throughout this experience.

Suttikiat Somvasoontra

# TABLE OF CONTENTS

**Page**

# LIST OF TABLES

**Page**

# LIST OF FIGURES

**Page**

# CHAPTER I INTRODUCTION

## Rationale and Significance of the Problem

Dental implants are the most common option for tooth replacement that enhances the oral health-related quality of life (OHRQoL)[1], especially in the esthetic area.[2] The single-tooth gap replacement in the anterior maxilla, maxillary central incisor, is challenging for the clinician in functional and esthetically outcomes. Numerous studies show the factors that affected the treatment outcomes in this area, including the correct three-dimensional position of the fixture, primary stability of the dental implant, and quantity of available bone.[3-5] Grunder et al.[6] recommended the minimum thickness of facial bone is two mm., preferably four mm. Kan et al. [7,8] classify the sagittal root position into four classes to evaluate the bone housing involved with implant therapy. Altogether, the alveolar bone thickness is an essential key factor in choosing the implant's design and placement.



World Population Aging 2019 defines "Elderly persons" as persons aged 65 years or over. Globally, the proportion of implant patients aged over 70 increased rapidly.[9,10] By 2050, 1 in 6 people will become elderly, up from 1 in 11 in 2019.[11] The world will become an aging society. Chronological age has been suggested as one of the risk factors for implant success. Some studies reported that age might be associated with a higher implant failure rate.[12,13] Aging was a factor in reducing the buccal bone wall of the anterior maxillary teeth.[14] On the other hand, sex

was also reported to have a negative linear correlation with the palatal bone thickness and significantly thinner bone wall in postmenopausal women.[15,16] Therefore, changes in the anterior maxillary alveolar bone thickness would be associated with age and sex difference.

In implant dentistry, the arch form of the maxilla influenced the prosthetic treatment plan, such as stress distribution around the dental implant, the number of implants, and the implant position.[13,14] In addition, several studies used the CBCT to find the relationship between bone quantity and various types of arch form, for example, alveolar arch form and dental arch form.[15,16] The database of bone quantity from the CBCT image files related to the clinical arch form may help predict the quantity of the alveolar bone.

Cone-beam computed tomography (CBCT) is a non-invasive and high-resolution imaging technique widely used in various dentistry fields, especially in planning implant surgeries.[17] CBCT is helpful to measure bone thickness. Three-dimensional(3D) images are not subject to distortion or affected by the surrounding structures' superposition. From the essential of alveolar bone thickness and accuracy of CBCT, Bulyalert et al.[18] recently reported the classification of the alveolar arch form in the maxillary anterior esthetic zone related to the alveolar bone thickness. In contrast, CBCT is unavailable for every dental hospital or private dental clinic.

Practically, due to the cost of the CBCT machine being still high, every dental clinic or hospital cannot provide for the clinician. Misch[19] presented the practical measurement methods to classify the dental arch form by measuring the distance of the anterior cantilever in the premaxilla area from the dental model or intraoral measurement. Additionally, the previous studies reported that tooth dimension and arch measurement accuracy and reliability using CBCT are clinically acceptable.[20,21] Therefore, this study used the CBCT imaging files to categorize the dental arch form.

Taken together, an in-detail understanding of alveolar bone thickness, dental arch form, and sagittal root position in the maxillary central incisor according to age and sex could help to predict the prognosis of implant treatment in this challenging area, then reduce the rate of a surgical complication, prosthetic complication, and esthetic complication.



Therefore, the objective of this study was to evaluate the association among the dental arch form, age-sex groups, and SRP regarding alveolar bone thickness in the maxillary central incisor using CBCT images, and the correlation between the predictor variables and alveolar bone thickness using cone-beam computed tomography (CBCT) images.

## Research Question

Is there any association among the dental arch form, age-sex groups, and sagittal root position (SRP) regarding alveolar bone thickness in the maxillary central incisor using cone-beam computed tomography (CBCT) images?

## Research Objectives

To find associate among the dental arch form, age-sex groups, and sagittal root position (SRP) regarding alveolar bone thickness in the maxillary central incisor using cone beam computed tomography (CBCT) images.

## Hypothesis

- Null Hypothesis ($H_0$)

There is no association among alveolar bone thickness, sagittal root position of maxillary central incisor tooth, and dental arch form by using CBCT images.

- Alternative Hypothesis ($H_1$)

There is an association among alveolar bone thickness, sagittal root position of maxillary central incisor tooth, and dental arch form by using CBCT images.

## Conceptual Framework

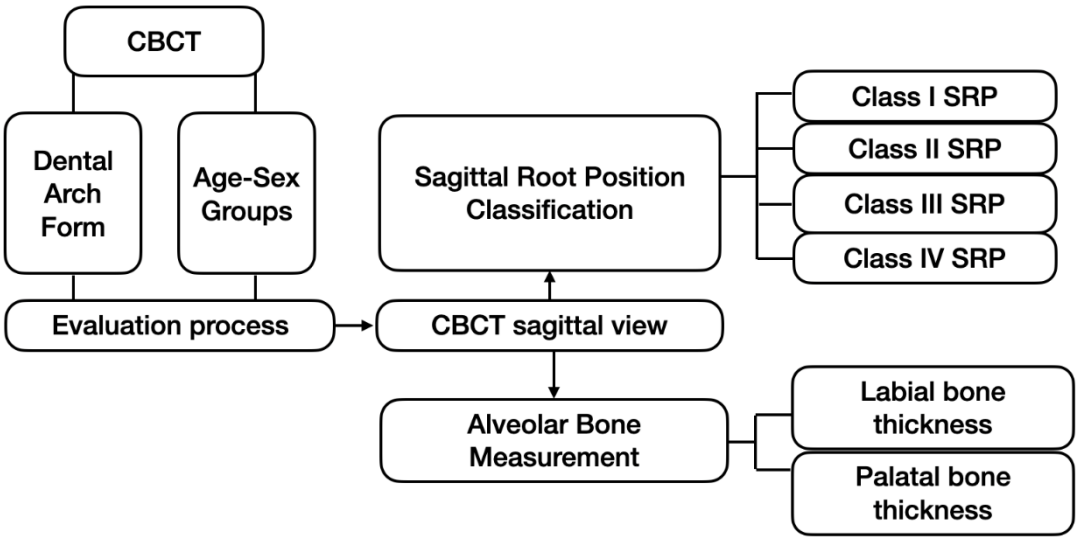


***Figure 1*** *The conceptual framework*

## Keywords

Dental Arch, Alveolar Process, Dental Implants, CBCT

## Expected benefit of the study

The outcome of this study will demonstrate the alternative method for classifying dental arch form intraorally, which can predict the information of alveolar bone thickness in the maxillary central incisor region, and also the relationship among the type of the dental arch form, class of the sagittal root position and the labio-palatal thickness of the anterior maxillary alveolar ridge at the maxillary central incisor area, including with the data of the sagittal root position in all age-sex groups. Moreover, a patient that does not require to use the cone beam computed tomography examination. This study will improve the communication of clinicians and patients to understand the anatomical consideration of each type of dental arch form, age-sex group.

## Ethical consideration

This study was conducted with the approval of the Ethical Committee at the Faculty of Dentistry, Chulalongkorn University, Bangkok, Thailand (HREC-DCU 2020-023).

# CHAPTER II REVIEW OF THE LITERATURE

## Arch form

The arch form was first introduced in 1932 by Chuck et al.[22], classified by the curvature of the arch as square, ovoid, and taper. In addition, the arch form was classified into three categories by the measurement method; alveolar arch form, basal arch form, and dental arch form.

The alveolar arch form was defined as the curvature of the alveolar bone that supports the dentition. In 2018, Bulyalert et al.[18] evaluated and classified arch form in the anterior esthetic region at the level of implant shoulder using CBCT images. The intercanine and interpremolar width, depth, and width/depth ratio values were also assessed. This study reported that the buccolingual alveolar bone thickness exhibited significant differences among the arch forms.



Peetaibunlue et al.[23] studied the relationship between maxillary anterior alveolar arch form and the tooth-root axis in class I occlusion. The studies were performed using the CBCT images by novel classification of the alveolar arch form of Bulyalert et al.[18] and the sagittal root position of Kan et al.[7]. This study concluded that both the sagittal root position and alveolar arch form were more predictive than individually. In addition, the basal arch form was defined as the curvature of a band of soft tissue superior to the mucogingival junction or the WALA ridge(Will

Andrews and Larry Andrews), but the soft tissue thickness among teeth varied might affect the positions of the WALA point.

The dental arch form was defined as the curvature of dentition. Many studies reported classifying the maxillary arch form or the dental arch form using measurements derived from models.[24,25] However, the existing report did not represent the intraoral approach. According to Carl E Misch[26], the dental arch form is determined by the distance from two horizontal lines. The first line is drawn from one canine's edge to the other. This line often bisects the incisive papilla regardless of the dental arch form. The second line is drawn parallel to the first line, along with the facial position of the anterior teeth. If the distance is 8 mm or less, the patient has a square arch form. If the distance is 8-12 mm., the patient has an ovoid dental arch form. If the distance is 12 mm or more, the patient has a tapering arch form. The dental arch form can be classified as keeping control without any bias from the numerical measuring approach. Additionally, The premaxilla anterior arch length showed no significant differences in various classes of malocclusion and sex differences.[27,28] It is hoped that this method will have possible clinical applications.



## Alveolar Bone Thickness

Spray et al.[29] reported that more significant amounts of facial bone loss were associated with implants that failed to integrate. As the bone thickness approached 2 mm, bone loss decreased

significantly, and some evidence of bone gain was seen. Grunder et al.[6] recommended that labial bone be required at least 2 mm. of thickness to provide stability, decrease marginal bone loss, prevent a gingival recession, and promote an esthetically favorable outcome after implant placement.

Numerous studies tried to quantitatively measure the labial bone thickness by a cone beam computed tomography, which usually found labial bone thickness thinner than 2 mm in the maxillary esthetic area. Hence, the palatal alveolar bone thickness seems to be an essential role to consider when deciding the implant's diameter, length, and taper design for providing the information for implant placement in the optimal position. Do et al.[15] are aware of the thinness of the palatal bone plate, as this could result in perforation of the palatal bone plate during surgical procedures associated with immediate maxillary implant placement in the Asian population. From their study, an increased buccolingual angulation of the maxillary lateral incisors was correlated with a thinner palatal bone plate at the apical level.



In addition to the alveolar bone thickness, Kan et al.[7] emphasize the importance of the buccolingual angulation of the anterior teeth when determining the appropriate treatment approach. Although various studies have measured the labial and palatal alveolar bone thickness, sagittal root position, and arch form, these correlations remain unclear.

**Sagittal Root Position**

Kan et al.[7] used CBCT images to classify the relationship of the anterior maxillary teeth' sagittal root positions(SRP) to their osseous housing. Class I was defined as the root was positioned against the labial cortical plate. Class II was centered in the middle of the osseous housing without engaging at the apical third of the root. Class III was positioned against the palatal cortical plate, and Class IV engaged both the labial and palatal cortical plates at least two-thirds of the root. The results showed that classes I, II, III, IV were found 81.1%, 6.5%, 0.7%, and 11.7%, respectively.

Wang et al.[30] were found that the facial bone wall in most maxillary anterior teeth was very thin. In addition, there was a significant sagittal angulation between the long axes of teeth and those of their respective alveolar bone in most esthetic zone positions.

Xu et al.[31] determined CBCT images to classify the relationship of the sagittal root position of the maxillary central incisor within the respective alveolar bone as buccal, middle, and palatal clinical significance in immediate implant placement and the buccal type was further classified into subtype I, II, and III according to buccal bone thickness. In 2017, Jung[32] used Xu's root position classification to classify and analyze the relationship of this classification, the buccal bone thickness, and the buccolingual angulation of the maxillary incisors using the CBCT images. The maxillary incisors' root was mainly located more buccally within the alveolar bone housing.

The buccal subtype III showed the greatest angulation, while the middle type showed the lowest angulation. Most of the maxillary incisors had a thin buccal bone wall, and the maxillary lateral incisor showed a greater angulation than the maxillary central incisor.

In contrast, Giglou et al.[33] showed that the majority of the roots in the anterior esthetic zone were positioned against the labial plate. Furthermore, there was no correlation between the sagittal root position and the thickness of buccal or palatal bone plate thickness that, contrary to some hypotheses that roots positioned along with the labial plate, will correlate with thinner labial bone plate thickness. Additionally, Peetaibunlue et al.[34] were reported that the clinician should account for both the alveolar arch form and SRP when planning implant placement procedures in this region, and the influence of SRP was more significant.

Therefore, the benefit of evaluated SRP in CBCT is helpful to treatment planning in immediate implant placement and increase the prosthetic option for implant prosthesis prior to the surgical approach visit.



## Implant position

Implant position needed to be considered in all three dimensions and concerning the adjacent teeth. The most challenging was the anterior maxilla, where a malposition might affect the treatment outcome. According to Chen et al.[35], the bone crestal area supports the mucosal shape of the alveolar process. The mucosal recession will likely develop if that bone is missing,

leading to esthetic complications. As a result, several authors recommended placing an implant no closer than 1.5 mm to the adjacent root surface in the mesiodistal dimension.[36,37] In the labiopalatal dimension, the implant shoulder was located 1 mm palatal to the point of the emergence at adjacent teeth, about 3 mm to the proposed gingival margin, or 1 mm to the cementoenamel junction of the adjacent teeth[38]

The study of Romeo et al.[39] reported that the single tooth implants exhibited a seven-year survival rate of 100% in the maxillary region under the standard anatomic condition. Hence, the single-tooth implant restorations would be a predictable treatment if the available bone was sufficient.

## Elderly Person

Many references classify the definition terms of "Elderly" or "Older person." These terms are from the United Nations (UN) [40], which agreed to cut off the patient who has more than 65 years old to refer to an older person. The number of older persons aged 60 years or elderly is expected to more than double by 2050 and more than triple by 2100. Globally, the population aged 60 or over is growing faster than all younger age groups[41,42], and women's longevity advantage over men leads to a predominately female older population.[40]

In Asia, While the countries or areas with the highest old-age dependency ratio(OADR) are predominantly European at present, more Asian countries and regions will be among this group

in 2050. Japan currently has the highest OADR in the world.[40] Thailand is ranked as having the second most rapidly growing aging population, being almost faster than that in developed countries.[43]

Several authors have discussed age as a prognostic factor in implant success in dental implant treatment, but it would not be a contraindication. In general, bone and soft tissue's reserved capacity makes it possible to establish osseointegration in the long run. Rather than aging itself, the specific nature of the disease process, such as osteoporosis and local bone quality and quantity at the implant site, mainly related to aging, is more critical for successful dental implant treatment.[12]

Changing in elderly patients, The structural elements of the shift in midface dramatically with age and, coupled with soft-tissue changes, lead to the appearance of the aged face. The bone mass density of the face changes with age, similar to the axial skeleton that may contribute to the presence of an aging face.[44,45] While the maxilla is more susceptible to age-related loss than the zygoma.[46] Mendelson et al.[47] confirmed the finding that the maxilla retruded with aging and quantitated the changes. Areas with a strong predisposition to resorption include the midface of the human skeleton, particularly the maxilla.

The maxillary bone density of subjects with osteoporosis is significantly lower than in healthy patients. Moreover, there is a direct correlation between the density of the skeleton and

the density of some maxilla sites. Using measurements of maxillary bone density will predict skeletal bone density that might be a valuable tool for the screening of osteoporosis.[48] Merbeb J et al.[49] reported that bone density and cortex thickness significantly influence the primary stability of the implant, which can be predicted based on a preoperative assessment of bone characteristics.

Abnormal absence of menstrual periods (amenorrhea), low estrogen level (menopause), and low testosterone levels in men can bring on osteoporosis. In addition, Zhang et al.2016[16] found that postmenopausal women versus older men have significantly different bone thicknesses. In contrast, premenopausal women versus younger men and younger men versus older men have no such differences. Therefore, when anterior implant planning, the aging condition is one concern factor.



**CBCT Evaluation**

Conventional techniques like periapical radiograph and panoramic radiograph were commonly used in many dentistry fields, including dental implants. Both radiographic techniques can display the information only in two-dimensional mesiodistal width and incisoapical height. In Implant planning, the Buccolingual dimension is needed. In the past, there was a ridge mapping technique to measure the underlying bone after local anesthesia. However, this technique is invasiveness and nonreliable.[50]

In 1998, Mozzo et al. introduced the Cone Beam Computed Tomography system.[51] CBCT provides reliable three-dimensional radiographic images that are beneficial for diagnosis and treatment planning like significantly lower radiation exposure, reasonably short scanning times, compact design together with adequate accuracy than conventional multislice computed tomography.[52] Studies relied on CBCT to assess the amount of alveolar bone at the interesting area to determine the surgical area.[53,54]

implantologists should have three-dimensional (3D) information of bone volume and topography prior to implant placement to improve implant therapy's overall success with a possible reduction in surgical and postoperative implant complications.[55] Therefore, the study of alveolar bone quantity and quality using CBCT is instantly increased due to the reliability and accuracy of the images and software.



The evaluation was performed mainly by using cementoenamel junction (CEJ) as the reference point and measuring the bone thickness at the various distances below CEJ. Since the crestal bone height of the natural teeth follows CEJ, facial bone is approximately located at 3 mm apical to the proximal bone.[56] Normally, the biological width at the facial aspect is about 3 mm. Hence, the implants should be placed 3 mm below the gingival margin or 2-3 mm apical to the CEJ of the adjacent teeth.[57]

Lee et al.[58] measured the thickness of the facial bone plate at 3 mm below the CEJ, 4.5 mm below the CEJ, mid root, and root apex in 2010. The correct location of the implant shoulder after placement is 3 mm below the CEJ, which has an impact on the cosmetic result since the bone in this area supports the appearance of marginal gingiva. In order to avoid alveolar plate perforation during the implantation procedure, information on bone thickness in other areas is useful.

However, there are few research on the labial and palatal bone thickness of maxillary central incisor teeth in relation to dental arch form especially in the elderly, where most patients have high expectations.

# CHAPTER III MATERIALS AND METHODS

## Materials

1. CBCT images of 280 patients have represented three types of the dental arch form (Misch C.E. 2015) analyzed from the computer database of ADTEC (Advanced Medical Devices Technology & Medical Robotics) Pathumthani, Thailand.

2. Scanner (Planmeca Promax® 3D Max, Planmeca, Helsinki, Finland ) with 400 voxel size (μm)

3. CBCT viewing software ( Planmeca Romexis Viewer Ver 5.2.0.R, Planmeca, Helsinki, Finland ) and ( Kodak Dental Imaging Software 3D Module 2.4, CodeWeavers Inc., Saint Paul, MN, USA )

## Methods

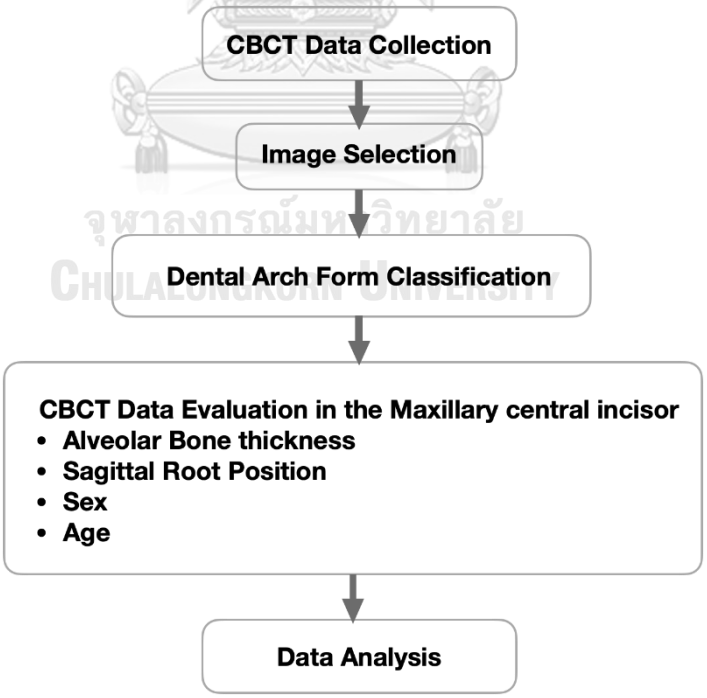


***Figure 2*** *Diagram of the study design*

**Image Selection**

CBCT images were taken from the patient's database of ADTEC (Advanced Medical Devices Technology & Medical Robotics). In addition, the data was obtained from the preoperative planning of posterior implant placement and orthodontic consultation between January 2018 to June 2020 that met the following criteria will be used as the samples of this study.

***Table 1*** *Inclusion and exclusion criteria for image selection*

| Inclusion Criteria | Exclusion Criteria |
|---|---|
| ▪ CBCT image without defects or artifacts<br>▪ They are remaining all anterior maxillary teeth.<br>▪ Patient's ages are greater than or equal to 20 years old ( ≥20 years old ) | ▪ History of orthodontic therapy<br>▪ Severe Attrition<br>▪ Presence of significant bone loss<br>▪ Anterior teeth were restored with a dental crown, dental implant, or dental post.<br>▪ Severe crowding on the upper anterior maxillary tooth<br>▪ Radiographic evidence of infection, severe root resorption, trauma, and surgical treatment |

## Data collection

The images were acquired using a CBCT scan ( Planmeca Promax® 3D Max, Planmeca, Helsinki, Finland ) with 400 voxel sizes (μm). The CBCT data were exported into digital imaging and communications in medicine (DICOM) files. All Dicom files in the patient's database were imported into CBCT viewing software ( Planmeca Romexis Viewer Ver 5.2.0.R, Planmeca, Helsinki, Finland ). Then used the CBCT image files, which meet all inclusion and exclusion criteria for dental arch classification.

After that, the selected image files will be evaluated by one examiner with the viewer ( Kodak Dental Imaging Software 3D Module 2.4, CodeWeavers Inc., Saint Paul, MN, USA ) for the alveolar bone thickness and sagittal root position. All data measurements were performed under 300 percent magnification by an examiner.

## Sample size description

The sample size was performed using the G*Power application based on 5% Type I Error and the 80% study power. The sample size from the calculation was 60 subjects for each group.



## Examiner Calibration

To standardize and ensure the consistency of measurement in this study. Intra-observer reliability will be performed by measuring the variables: square arch form, ovoid arch form, taper arch form, labial bone thickness, palatal bone thickness, sagittal root position class I, II, III, and IV in the maxillary central incisor teeth from 28 CBCT images. The following measurement will be settled four weeks apart from the previous one. The results from each measurement will be evaluated for the intraclass correlation coefficient (ICC).

**Dental arch form measurement and classification**

The classification and the measurement of dental arch form were briefly explained and cited from Misch, C.E.[19] The distance from two horizontal lines measured the premaxilla dental arch forms. The first line draws from the tip of one canine to the other. This line most often bisects the incisive papilla. Another line is drawn parallel to the first line and the facial surface of the anterior teeth. The vertical line was drawn perpendicular to both horizontal lines. It can show the length between two horizontal lines and represent the cantilever distance in millimeters.

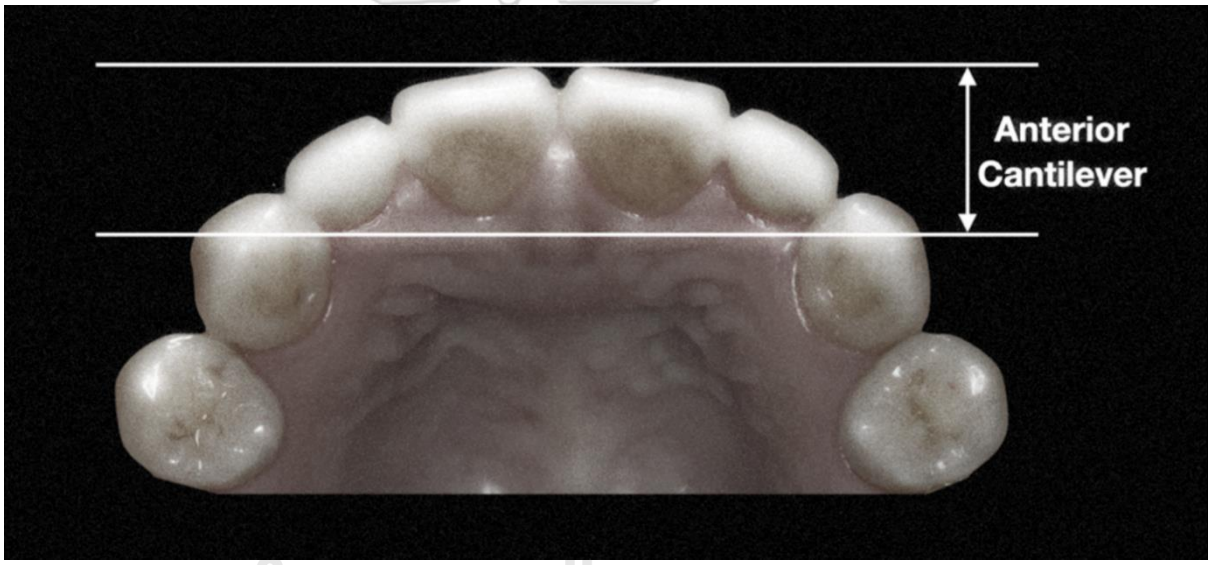




***Figure 3*** *Anterior cantilever distance (mm) between two imaginary horizontal lines, as reported by Misch C.E.*[19]

A square dental arch form is present when the distance between these two lines is less than 8 mm. When the distance between these two lines is 8 to 12 mm, the ovoid dentate arch form is present. When the distance between the two horizontal lines is greater than 12 mm, the dentate arch form is tapering.

***Table 2*** *Definition of Dental arch form variables*

| Variables | Definition |
|---|---|
| Square arch form | the distance is 8 or less. |
| Ovoid arch form | the distance is 8-12 mm. |
| Taper arch form | the distance is 12 mm. or greater. |

According to the previous study about CBCT accuracy[21], determining mesiodistal tooth size, intercanine width, intermolar distance, and arch length quickly, precisely, reliably, and reproducibly compared with the measurement obtained using the digital method on digitalized plaster models. Furthermore, the differences existing between both methods are clinically acceptable. Therefore, this study uses the 3D rendering views to locate the tip of both maxillary canines.

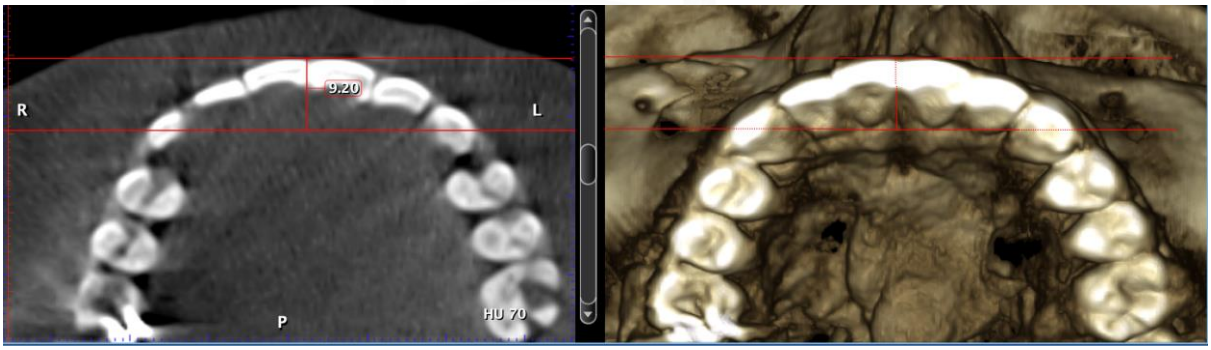


***Figure 4*** *Dental arch form classification from the axial view and 3D rendering view*

**The alveolar bone thickness measurement**

The labial and palatal thickness of the alveolar bone was measured according to the report of DO et al.[15] with minor modifications. The DICOM files were imported into CBCT viewing software (Kodak Dental Imaging Software 3D Module 2.4, CodeWeavers Inc., Saint Paul, MN, USA). All CBCT images were sliced at the positions of each maxillary central incisor. Thus, all sliced images of the maxillary central incisors were used for alveolar bone thickness measurement. The axes of the teeth were set perpendicular to the labial contour of the alveolar bone, passing through the center of the root canal in the coronal plane (Fig. 5).

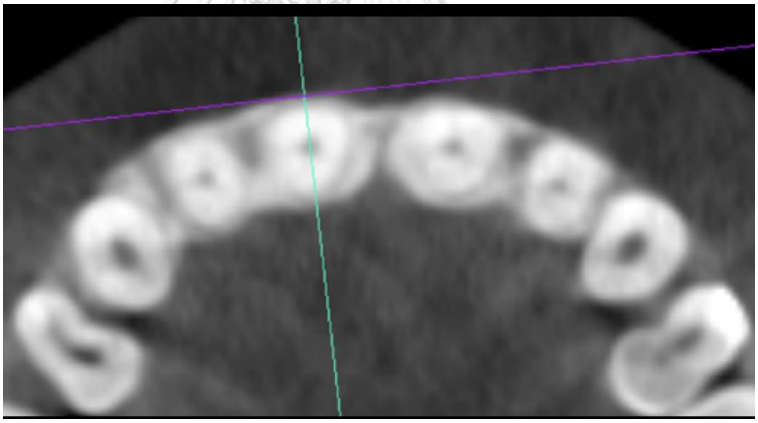

***Figure 5*** *The labial and palatal bone thickness were measured perpendicular to the alveolar cortical bone from the central slice sagitally*

In the sagittal view, the three reference planes perpendicular to the long axis of the root were drawn at 3 mm below CEJ: LiPi plane, root apex: LaPa plane, and mid-root (the plane at the middle of the distance from LiPi plane to LaPa plane): LmPm plane.

Then, the bone thickness of the labial and palatal alveolar bone were measured at seven areas:

(i) labial alveolar bone thickness at 3 mm apically from CEJ (Li)

(ii) labial bone thickness at 3 mm apically from CEJ (Pi)

(iii) labial alveolar bone thickness at the root apex level (La)

(iv) palatal alveolar bone thickness at the root apex level (Pa)

(v) alveolar bone thickness at the root apex level (LaPa)

(vi) labial alveolar bone thickness at the mid-root (middle distance of 3 mm apically from the CEJ to the root apex level) (Lm)

(vii) palatal alveolar bone thickness at the mid-root (middle distance of 3 mm apically from the CEJ to the root apex level) (Pm)

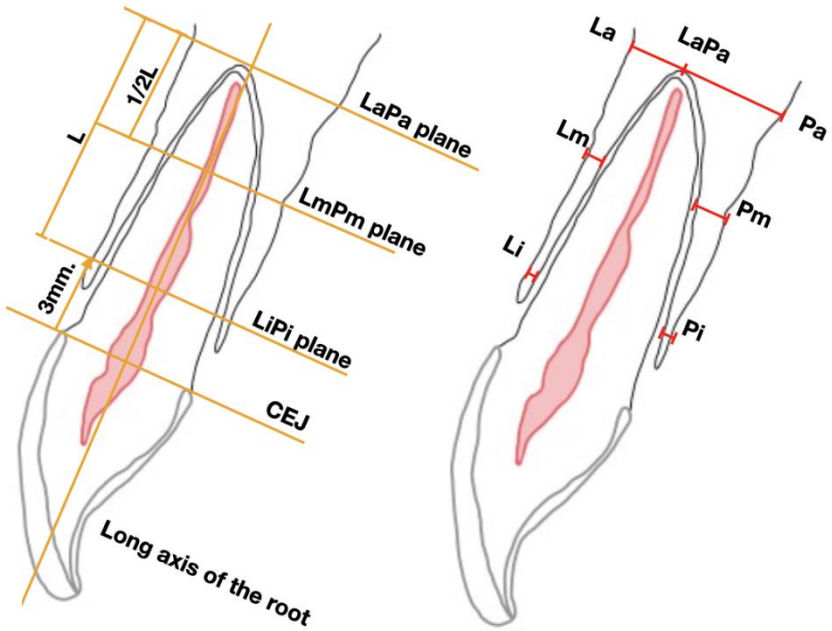


***Figure 6*** *Alveolar bone thickness measurement in 7 areas*

## Sagittal Root Position Classification

Sagittal root position (SRP) was defined based on the type of dental root position of the maxillary central incisors and alveolar bone housing. CBCT images were classified according to the SRP classification reported by Kan et al.[7], which divided the tooth root position within its bone into four classes, including class I, II, III, and IV, as detailed in Figure 5. SRP class I include the root was engaged with the buccal cortical bone. SRP class II, the root was in the middle of the alveolar bone housing without engaging either the buccal or the palatal bone at the apical third of the root. SRP class III, the root was engaged with the palatal cortical bone. Finally, SRP class IV, the root was engaged to either the buccal or the palatal cortical bone.

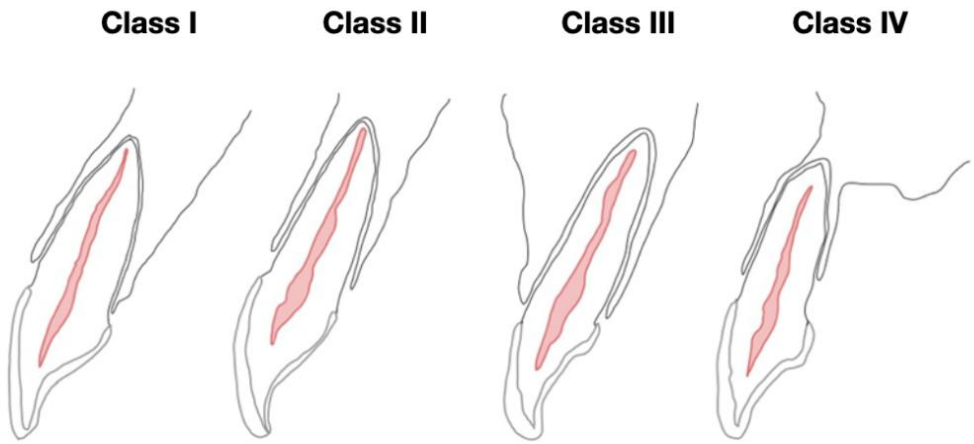


***Figure 7*** *The sagittal root position classification reported by Kan et al.*[7]

**Data Analysis**

The data were analyzed using statistical software (SPSS 22.0, SPSS, Chicago, IL, USA). Chi-square was used to find the association of the dental arch form with sex, age group, age-sex groups, and SRP. The median and interquartile range of the alveolar bone thickness were calculated according to the different dental arch forms, age-sex groups, and SRP. The normality of the data was determined by the Kolmogorov Smirnov test, while the Kruskal-Wallis test assessed the relationship between dental arch form and alveolar bone thickness or sagittal root position. The multiple regression model was performed to determine which predictor variables can affect the thickness of the alveolar bone. $P < 0.05$ was set as statistically significant differences.

# CHAPTER IV RESULT

In the present study, 560 CBCT images of left and right maxillary central incisors from 280 patients (122 male, 158 female) meet this study's criteria evaluated. In addition, their age range is from 20 to 81 years (average age, 55 years). According to Carl E Misch[19], the classification of the dental arch forms was evaluated and analyzed from 3D-rendering in the CBCT image viewer. As a result, there were 80 Square arches, 135 Oval arches, and 65 Taper arches. However, no statistical difference was found between dental arch forms in each age group, sex, and age-sex group.

Table 3 indicates the dental arch form does not differ significantly between the age group, sex, and age-sex group (P=.446, P=.193, and .433, respectively). The most common arch form is the oval arch form (48.3%). Meanwhile, the taper arch form is the least (23.2%). In addition, the distribution of age-sex group in each dental arch form is an equal proportion (P >.05).

***Table 3*** *Dental arch form distribution (percentage) according to age group, sex, and age-sex groups*

| Variables | | Total n=280 | Dental arch form | | | P-value* |
|---|---|---|---|---|---|---|
| | | | Square arch form n=80 (28.5%) | Oval arch form n=135 (48.3%) | Taper arch form n=65 (23.2%) | |
| Age group | Adult (≥ 20-64 y) | 179 (63.9%) | 52 (29.1%) | 80 (44.7%) | 47 (26.3%) | .446 |
| | Elder (≥ 65 y) | 101 (36.1%) | 28 (27.7%) | 55 (54.5%) | 18 (17.8%) | |
| Sex | Male | 122 (43.6%) | 36 (29.5%) | 54 (44.3%) | 32 (26.2%) | .193 |
| | Female | 158 (56.4%) | 44 (27.8%) | 81 (51.3%) | 33 (20.9%) | |
| Age-sex group | Adult male | 74 (26.4%) | 23 (30.1%) | 28 (38.4%) | 23 (31.5%) | .433 |
| | Elderly male | 49 (17.5%) | 14 (28.6%) | 26 (53.1%) | 9 (18.4%) | |
| | Adult female | 105 (37.5%) | 29 (28.3%) | 52 (49.1%) | 24 (22.6%) | |
| | Elderly female | 52 (18.6%) | 14 (26.9%) | 29 (55.8%) | 9 (17.3%) | |

* P-value indicates no significant differences between dental arch form and age group, sex, or age-sex group, analyzed using chi-square (P-value >.05).

According to Kan et al.[7], SRP was categorized into four classes. The number of SRP classes I, II, III, and IV in this study are shown in Table 4. Statistical analysis shows that the dental arch form and SRP distribution are not associated with each other. The data shows that more than 96.4% of the maxillary central incisor was aligned buccally within the labial bone (Class I). In contrast, the maxillary central incisor teeth were not found in which the root engaged with the palatal cortical bone (Class III). Similarly, the sagittal root position was equally distributed in each arch form, as shown in Table 4,

***Table 4*** *Dental arch form distribution (percentage) according to sagittal root position*

| | | Total | Dental Arch Form | | | P-value* |
|---|---|---|---|---|---|---|
| | | | Square Arch Form n(%) | Oval Arch Form n(%) | Taper Arch Form n(%) | |
| SRP | Class I | 540(96.4%) | 156(28.9%) | 258(47.8%) | 126(23.3%) | .283 |
| | Class II | 17(3.0%) | 2(11.8%) | 11(64.7%) | 4(23.5%) | |
| | Class III | 0(0.0%) | 0(0.0%) | 0(0.0%) | 0(0.0%) | |
| | Class IV | 3(0.6%) | 2(66.7%) | 1(33.3%) | 0(0.0%) | |
| | Total | 560(100%) | 160(28.6%) | 270(48.2%) | 130(23.2%) | |

SRP, sagittal root position

* P-value indicates no significant differences between dental arch form and sagittal root position, analyzed using chi-square (P-value >.05).

The median and interquartile (IQR) range of all variables area in each dental arch form were presented in Table 5. Four variables (Pi, Lm, La, Pa areas) showed a significant difference among the dental arch form (P-value <.05). The square arch had the most significant palatal alveolar bone thickness at the root apex, followed by the oval arch and the taper arch forms. While the Li, Pm, and LaPa are not different median and interquartile across the dental arch form (P-value >.05).

***Table 5*** *Comparison of the median and interquartile range (IQR) of alveolar bone thickness among the dental arch form*

| n=560 | Dental Arch Form | | | P-value |
|---|---|---|---|---|
| | Square Arch Form n=160 | Oval Arch Form n=270 | Taper Arch Form n=130 | |
| Li | 0.70(0.50-1.00) | 0.80(0.50-1.00) | 0.90(0.60-1.10) | .094 |
| Pi | 1.30(1.00-1.80) | 1.40(1.00-1.80)[a] | 1.20(0.90-1.70)[a] | .032* |
| Lm | 0.80(0.60-1.00) | 0.70(0.50-1.00)[a] | 0.90(0.60-1.10)[a] | .005* |
| Pm | 3.80(3.10-4.90) | 3.60(2.98-4.70) | 3.55(2.68-4.53) | .083 |
| La | 1.45(1.02-2.10)[a] | 1.60(1.10-2.20) | 1.90(1.30-2.40)[a] | .001* |
| Pa | 8.80(7.23-10.30)[a,b] | 8.00(6.68-9.50)[b] | 8.05(6.50-9.43)[a] | .003* |
| LaPa | 10.35(8.70-11.78) | 9.80(8.50-11.30) | 9.80(8.57-11.25) | .087 |

Li, Labial alveolar bone thickness at 3 mm apically from CEJ; Pi, Palatal alveolar bone thickness at 3 mm apically from CEJ; Lm, Labial alveolar bone thickness at the mid-root (middle distance of 3 mm apically from the CEJ to the root apex level); La, Labial alveolar bone thickness at the root apex level; Pm, Palatal alveolar bone thickness at the mid-root (middle distance of 3 mm apically from the CEJ to the root apex level); La, Labial alveolar bone thickness at the root apex level; Pa, Palatal alveolar bone thickness at the root apex level; LaPa, Alveolar bone thickness at the root apex level.

[*] Significant Differences among the dental arch form groups, analyzed using Kruskal-Wallis's test (P-value <.05)

[a,b] Horizontally, the same superscript letter indicates significant differences in alveolar bone thickness between groups, analyzed using Dunn's post hoc test. (P-value <.05).

In table 6, the highest median of bone thickness is the Pa area in SRP Class I, followed by Class II and IV, respectively. Every variable area showed statistically significant differences among the class. Only the Li did not show statistically significant differences among the class. Many variable areas in Class I SRP have presented the highest median of the thickness of bone except for the labial area (Li, Lm, and La areas). In Class II SRP, the Lm and La area showed the median of bone thickness highest than the other class. Additionally, the LaPa area showed statistically significant differences among the class that Class IV showed the lowest median of bone thickness (6.40).

As shown in this table 7, alveolar bone thickness showed statistically significant differences among the age-sex group in all variable. The elderly female group is showed a statistically significant differences between all age groups and presents the lowest alveolar bone thickness in all area. At Pa, the adult female showed the lower alveolar bone thickness but not significantly between groups. At Li and Pi, adult female and elderly female showed statistically significant difference alveolar bone thickness between groups. At Lm and La, the elderly female group has shown the statistical significance of alveolar bone thickness in all age groups. In contrast, there is no statistical difference between the adult male and elderly male group. Simultaneously, the Li of the adult male does not show any statistically significant differences

from the other groups. The Pa and LaPa have shown the similarity of statistical significance of median bone thickness in the same relation.

***Table 6*** *Comparison of the median and interquartile range (IQR) of alveolar bone thickness among sagittal root position*

| N=560 | Sagittal Root Position (SRP) | | | | P-value |
|---|---|---|---|---|---|
| | Class I<br>n=540 | Class II<br>n=17 | Class III<br>n=0 | Class IV<br>n=3 | |
| Li | 0.80(0.50-1.20) | 1.20(0.70-1.30) | - | 0.50(0.25-0.85**) | .054 |
| Pi | 1.40(1.00-1.80)[a] | 1.20(0.90-1.55) | - | 0.50(0.25-0.60**)[a] | .009* |
| Lm | 0.70(0.60-1.00)[a] | 1.30(0.90-1.65)[a] | - | 1.10(1.05-1.20**) | <.001* |
| Pm | 3.75(3.00-4.80)[a,b] | 2.80(2.00-3.90)[a] | - | 1.00(0.75-1.00**)[b] | <.001* |
| La | 1.60(1.10-2.18[a,b] | 3.50(3.00-4.35)[a] | - | 3.00(3.00-3.15**)[b] | <.001* |
| Pa | 8.20(6.90-9.70)[a,b] | 6.20(5.35-7.80)[a] | - | 3.40(3.00-3.70**)[b] | <.001* |
| LaPa | 10.00(8.60-11.40) [a] | 10.70(7.40-11.95)[b] | - | 6.40(6.00-6.85**)[a,b] | .021* |

Li, Labial alveolar bone thickness at 3 mm apically from CEJ; Pi, Palatal alveolar bone thickness at 3 mm apically from CEJ; Lm, Labial alveolar bone thickness at the mid-root (middle distance of 3 mm apically from the CEJ to the root apex level); La, Labial alveolar bone thickness at the root apex level; Pm, Palatal alveolar bone thickness at the mid-root (middle distance of 3 mm apically from the CEJ to the root apex level); La, Labial alveolar bone thickness at the root apex level; Pa, Palatal alveolar bone thickness at the root apex level; LaPa, Alveolar bone thickness at the root apex level.

[*] Significant Differences among the dental arch form groups, analyzed using Kruskal-Wallis's test (P-value <.05)

[a,b] Horizontally, the same superscript letter indicates significant differences in alveolar bone thickness between groups, analyzed using Dunn's post hoc test. (P-value <.05).

[**] interquartile range (IQR), analyzed using Tukey's Hinges

***Table 7*** *Comparison of the median and interquartile range (IQR) of alveolar bone thickness among age-sex groups*

| n=560 | Age-sex group | | | | P-value |
|---|---|---|---|---|---|
| | Adult Male n=148 | Elderly Male n=98 | Adult Female n=210 | Elderly Female n=104 | |
| Li | 0.80(0.50-1.20) | 0.70(0.50-1.10)[a] | 0.90(0.60-1.30)[a,b] | 0.70(0.50-1.00)[b] | .002* |
| Pi | 1.40(1.00-1.90)[a] | 1.40(1.00-1.80) | 1.40(1.10-1.80)[b] | 1.20(0.90-1.60)[a,b] | .007* |
| Lm | 0.90(0.70-1.20)[a] | 0.80(0.60-1.10)[b] | 0.70(0.60-1.00)[c] | 0.60(0.50-0.88)[a,b,c] | <.001* |
| Pm | 4.25(3.20-5.33)[a,b] | 4.20(3.30-5.30)[c,d] | 3.40(2.82-4.20)[a,c] | 3.30(2.70-4.20)[b,d] | <.001* |
| La | 2.00(1.30-2.30)[a,b] | 1.80(1.30-2.40)[c] | 1.60(1.10-2.20)[a,d] | 1.30(0.90-1.70)[b,c,d] | <.001* |
| Pa | 8.90(7.50-10.50)[a,b] | 9.20(8.00-10.83)[c,d] | 7.40(6.30-8.70)[a,c] | 7.55(6.43-9.25)[b,d] | <.001* |
| LaPa | 10.90(9.70-12.60)[a,b] | 11.10(10.08-12.50)[c,d] | 9.20(8.20-10.50)[a,c] | 9.10(8.10-10.40)[b,d] | <.001* |

Li, Labial alveolar bone thickness at 3 mm apically from CEJ; Pi, Palatal alveolar bone thickness at 3 mm apically from CEJ; Lm, Labial alveolar bone thickness at the mid-root (middle distance of 3 mm apically from the CEJ to the root apex level); La, Labial alveolar bone thickness at the root apex level; Pm, Palatal alveolar bone thickness at the mid-root (middle distance of 3 mm apically from the CEJ to the root apex level); La, Labial alveolar bone thickness at the root apex level; Pa, Palatal alveolar bone thickness at the root apex level; LaPa, Alveolar bone thickness at the root apex level.

* Significant Differences among the dental arch form groups, analyzed using Kruskal-Wallis's test (P-value <.05)

[a,b,c,d] Horizontally, the same superscript letter indicates significant differences in alveolar bone thickness between groups, analyzed using Dunn's post hoc test. (P-value <.05).

Based on the results from this study comparisons, The types of the dental arch form, SRP classifications, and age-sex groups were significantly associated with alveolar bone thickness. Therefore, the following three factors were included in the linear regression model: 1) types of the dental arch form, 2) SRP classifications, and 3) age-sex groups. In the univariate model (table 8), at the Li, the significant negative correlation is shown in the square arch form (-.089, p<.1) and elderly female (-.142, p<. 05) while the significant positive correlation is shown in the class II SRP (.227, p<.05). At the Pi, the significant negative correlation is shown in the taper arch form, class IV SRP, and elderly females (-.179, -1.049, -.265, p<.05, respectively). At the Lm, the significant negative correlation is shown in the elderly female (-.241, p<.05), while the significant positive correlation is shown in the taper arch form (.126, p<.05) and class II SRP (.450, p<.05). At the Pm, the significant negative correlation is shown in the class II SRP, class IV SRP, adult female and elderly female (-1.055, -3.110, -.788, -.905, p<.05, respectively) while the arch form showed no significant correlation in alveolar bone thickness of Pm. At La, the significant negative correlation is shown in the square arch form, adult female and elderly female (-.173, -.205, -.590, p<. 05), while the significant positive correlation is shown in the taper arch form, class II SRP and class IV SRP. (.183, 1.909, 1.420, p<.05). At Pa, the significant negative correlation is shown in the class II SRP, class IV SRP, adult female, and elderly female (-2.005, -5.142, -1.397, -1.168, p<.05, respectively) while the significant positive correlation is shown in the square arch form. At the

LaPa, the significant negative correlation is shown in the class IV SRP, adult female and elderly female (-3.722, -1.602, -1.758, p<.05, respectively), while the significant positive correlation is shown in the square arch form (.423, p<.1). The variable with p-value <.1 in the univariate analysis were simultaneously considered in the multivariate analysis. Therefore, SRP classifications and age-sex groups were used in the multivariate model of Pm, as shown in table 9.

The multiple linear regression model compared the alveolar bone thickness and predicted variables. At Li, those regression coefficients (β) demonstrated a significantly negative correlation in the elderly female (-.139, p<.05). The highest beta was shown in the elderly female (-.107, p<.05), followed by the square arch form (-.079, p<.05). At Pi, the significant negative correlation is shown in the taper arch form, class II SRP, Class IV SRP, and elderly female (-.221, -.331, -1.147, -.333, p<.05, respectively). The highest beta was shown in the elderly female (-.190, p<.05), followed by the taper arch form (-.137, p<.05). At La, the significant negative correlation is shown in the square arch form and elderly females (-.153, -.455, p<.05, respectively), while the significant positive correlation is shown in the taper arch form, class II SRP, and class IV SRP. The highest beta was shown in the class II SRP (-.190, p<.05), followed by the elderly female ( -.214, p<.05). At Pa, the significant negative correlation is shown in the class II SRP, class IV SRP, adult female, and elderly female (-2.114, -5.698, -1.532, -1.377, p<.05), while the significant positive

correlation is shown in the square arch form. The highest beta was shown in the adult female (-.335, p<.05), followed by the elderly female (-.242, p<.05). At Lm, the significant negative correlation is shown in the elderly female (-.196, p<.05), while the significant positive correlation is shown in the taper arch form and class II SRP (.119, .438, p<.05, respectively). The highest beta was shown in the elderly female (-.201, p<.05), followed by class II SRP (.198, p<.05). At Pm, the significant negative correlation is shown in the class II SRP, class IV SRP, adult female, and elderly female (-1.215, -3.348, -.858, -1.014, p<.05, respectively). The highest beta was shown in the adult female (-.288, p<.05), followed by the elderly female (.273, p<.05). At LaPa, the significant negative correlation is shown in the class IV SRP, adult female, and elderly female. The highest beta was shown in the adult female (-.370, p<.05), followed by the elderly female (.329, p<.05).

Compared to the alveolar bone thickness of the oval arch form, those in the square arch form demonstrated the significantly negative correlation of La (-.153, p<.05) while demonstrating the significant positive correlation of Pa (.520, p<.05). On the other hand, the taper arch form demonstrated the negative correlation of Pi (-.221, p<.05) while demonstrating the significant positive correlation of La and Lm (.174, .119, p<.05, respectively).



When comparing the alveolar bone thickness of class I SRP, those in class II SRP demonstrated the significantly negative correlation of Pi, Pa, and Pm (-.331, -2.114, -1.215, p<0.05) while demonstrating the significant positive correlation of La and Lm (1.827, .438, p<0.05). On the

other hand, in class IV SRP, the significantly negative correlation is shown in Pi, Pa, Pm, and LaPa (-1.147, -5.698, -3.348, -4.260, $p<0.05$) while demonstrating the significant positive correlation of La.

In terms of age-sex groups, compared to the alveolar bone thickness of the male adult, those in the adult female exhibited a significantly negative correlation is shown in Pa, Pm, and LaPa (-1.532, -.858, -1.651, $p<.05$, respectively). In addition, those in the elderly female exhibited a significant negative correlation of Li, Pi, La, Pa, Lm, Pm, and LaPa (-.139, -.333, -.455, -1.377, -.196, -1.014, -1.832, $p<.05$, respectively)

In term of standardized coefficient, beta, those in the elderly female exhibited the most value at Li, Pi, and Lm. In the adult female showed the most value at Pm, Pa and LaPa. At La, the SRP variable showed the most standardized coefficient values.



The $R^2$ between the predictor's variable and the alveolar bone thickness was ranked from La, LaPa, Pa, Pm, Lm, Pi, and Li (.237, .198, .192, .136, .110, .056, .039, respectively), were shown in Table 9.

***Table 8*** *Linear regression analysis for the association between the alveolar bone thickness and predicted variables*

| Predictor Variables | Li | | Pi | | Lm | | Pm | | La | | Pa | | LaPa | |
|---|---|---|---|---|---|---|---|---|---|---|---|---|---|---|
| | β(se) | *p* | β(se) | *p* | β(se) | *p* | β(se) | *p* | β(se) | *p* | β(se) | *p* | β(se) | *p* |
| Dental Arch Form | | | | | | | | | | | | | | |
| Square Arch Form | -.089(.050) | .076* | -.103(.068) | .131 | .046(.038) | .218 | .077(.144) | .593 | -.173(.082) | .034* | .597(.220) | .007* | .423(.216) | .050* |
| Taper Arch Form | .013(.054) | .813 | -.179(.073) | .014* | .126(.040) | .002* | -.244(.154) | .114 | .183(.087) | .037* | -.099(.235) | .674 | .084(.231) | .715 |
| SRP | | | | | | | | | | | | | | |
| Class II | .227(.124) | .067* | -.249(.167) | .137 | .450(.092) | <.001* | -1.055(.349) | .003* | 1.909(.186) | <.001* | -2.005(.533) | <.001* | -.096(.530) | .856 |
| Class IV | -.276(.291) | .343 | -1.049(.393) | .008* | .319(.215) | .139 | -3.110(.821) | <.001* | 1.420(.437) | .001* | -5.142(1.252) | <.001* | -3.722(1.245) | .003* |
| Age-sex groups | | | | | | | | | | | | | | |
| Elderly male | -.091(.065) | .165 | -.074(.088) | .406 | .015(.048) | .751 | .082(.181) | .650 | -.070(.105) | .505 | .408(.273) | .136 | .338(.258) | .191 |
| Adult female | .068(.054) | .206 | -.034(.073) | .642 | -.074(.040) | .065 | -.788(.149) | <.001* | -.205(.087) | .018* | -1.397(.225) | <.001* | -1.602(.212) | <.001* |
| Elderly female | -.142(.064) | .027* | -.265(.087) | .002* | -.241(.047) | <.001* | -.905(.178) | <.001* | -.590(.103) | <.001* | -1.168(.268) | <.001* | -1.758(.253) | <.001* |

Li, Labial alveolar bone thickness at 3 mm apically from CEJ; Pi, Palatal alveolar bone thickness at 3 mm apically from CEJ; Lm, Labial alveolar bone thickness at the mid-root (middle distance of 3 mm apically from the CEJ to the root apex level); La, Labial alveolar bone thickness at the root apex level; Pm, Palatal alveolar bone thickness at the mid-root (middle distance of 3 mm apically from the CEJ to the root apex level); La, Labial alveolar bone thickness at the root apex level; Pa, Palatal alveolar bone thickness at the root apex level; LaPa, Alveolar bone thickness at the root apex level.

β, the unstandardized coefficient; se, standard error; SRP, Sagittal Root Position

Oval Arch Form, Sagittal Root Position Class I, Adult Male were the reference group

*The variable with a P value <.1 in the univariate analysis were simultaneously considered in the multivariate analysis.

***Table 9*** *Multiple Linear regression analysis for the association between the alveolar bone thickness and predicted variables*

| Predictor Variables | Li | | Pi | | Lm | | Pm | | La | | Pa | | LaPa | |
|---|---|---|---|---|---|---|---|---|---|---|---|---|---|---|
| | β | Beta | β | Beta | β | Beta | β | Beta | β | Beta | β | Beta | β | Beta |
| Dental arch form | | | | | | | | | | | | | | |
| Square arch form | -.088 | -.079 | -.118 | -.078 | .049 | .058 | - | - | -.153* | -.083 | .520* | .106 | .367 | .077 |
| Taper arch form | -.001 | -.001 | -.221* | -.137 | .119* | .133 | - | - | .174* | .089 | -.260 | -.050 | -.087 | -.017 |
| Sagittal root position | | | | | | | | | | | | | | |
| Class II | .185 | .063 | -.331* | -.083 | .438* | .198 | -1.215* | -.144 | 1.827* | .379 | -2.114* | -.164 | -.288 | -.023 |
| Class IV | -.282 | -.041 | -1.147* | -.123 | .299 | .058 | -3.348* | -.169 | 1.438* | .127 | -5.698* | -.188 | -4.260* | -.144 |
| Age-sex groups | | | | | | | | | | | | | | |
| Elderly male | -.086 | -.065 | -.137 | -.076 | .058 | .059 | -.026 | -.007 | .064 | .029 | .195 | .033 | .259 | .046 |
| Adult female | .070 | .067 | -.077 | -.055 | -.045 | -.057 | -.858* | -.288 | -.119 | -.069 | -1.532* | -.335 | -1.651* | -.370 |
| Elderly female | -.139* | -.107 | -.333* | -.190 | -.196* | -.201 | -1.014* | -.273 | -.455* | -.214 | -1.377* | -.242 | -1.832* | -.329 |
| Constant | .884* | | 1.652* | | .817* | | 4.467* | | 1.804* | | 9.195* | | 10.999* | |
| $R^2$ | .039* | | .056* | | .110* | | .136* | | .237* | | .192* | | .198* | |
| P-value | .002 | | <.001 | | <.001 | | <.001 | | <.001 | | <.001 | | <.001 | |

Li, Labial alveolar bone thickness at 3 mm apically from CEJ; Pi, Palatal alveolar bone thickness at 3 mm apically from CEJ; Lm, Labial alveolar bone thickness at the mid-root (middle distance of 3 mm apically from the CEJ to the root apex level); La, Labial alveolar bone thickness at the root apex level; Pm, Palatal alveolar bone thickness at the mid-root (middle distance of 3 mm apically from the CEJ to the root apex level); La, Labial alveolar bone thickness at the root apex level; Pa, Palatal alveolar bone thickness at the root apex level; LaPa, Alveolar bone thickness at the root apex level. β, the unstandardized coefficient; se, standard error; SRP, Sagittal Root Position; Beta, Standardized coefficient Oval Arch Form, Sagittal Root Position Class I, Adult Male were the reference group, *P-value <.05

# CHAPTER V DISCUSSION

This study evaluated the association among the dental arch form, age-sex groups, and SRP regarding alveolar bone thickness in the maxillary central incisor using CBCT images. Most studies reported that arch form was categorized in several levels: alveolar bone level, basal bone level, and tooth level.[13,15,16,23,24] Practically, the premaxilla dental arch form can be classified from the intraoral examination or stone model without using the arch form template or mathematical calculation.[13,14,17] Therefore, the possibility of utilizing arch form would be more practical. To the best of our knowledge, this was the first study that used the classification of the dental arch form in the premaxilla area to characterize the alveolar bone thickness and SRP.

In this study, the CBCT 3D model was used for the types of dental arch form. The benefits of the CBCT 3D models are reproducible, cost-effective, and easy to manipulate data. Many reports showed the good accuracy and reliability of the linear measurement on the CBCT 3D model and clinically acceptable arch length and tooth size measurement.[20,21] There was no difference in the CBCT 3D model, digitalized model, or stone model's accuracy.[24,25] However, some studies found the dental arch dimension measurement variation as the reference point at the canine cusp tip might be a discrepancy from the canine's marginal ridge or anatomical tooth wear at the functional occlusal plane level.[21] Thus, to represent the actual cusp tip on the CBCT

image, the axial plane sliced to the most obvious point of both canine cusp tips was modified. This study used the intraclass correlation coefficient to find the reliability of the arch form measurement and showed almost perfect agreement. In our study, dental arch forms have been classified into square, oval, and taper. Previous studies demonstrated that the oval arch form was the most prevalent, similar to the result of our study.[22] On the other hand, the other types of dental arch form showed the most frequency in some studies.[18,23] The most common dental arch form was the oval arch form, square arch form, and taper arch form, respectively.

In single tooth replacement of the maxillary central incisor, the practitioner needs to replicate the tooth morphology and gingival margin concerning CEJ of the contralateral tooth. The previous research suggested placing the implant platform 3-4 mm below the gingival margin for the best esthetic result.[2,26] Our study determined the reference plane for the measurement at the pre-determined restorative margin level (3 mm from CEJ) related to the apex level. The availability of bone apical and palatal could represent the alveolar bone thickness at the appropriate implant position for the immediate implant placement approach according to the recommendation by Morton et al.[3]



Several studies focused on the alveolar bone thickness, including the labial and palatal aspects. Spray et al.[29] stated that the critical thickness value that reduces facial bone loss is around 2 mm on the labial aspect. Grunder et al.[4] also suggested that facial bone thickness

should be at least 2 mm to provide implant stability and achieve a long-term esthetic outcome. In many studies, most cases showed that the labial bone wall of the anterior maxillary teeth was very thin.[27,28] Similarly, our study showed a thin and less than 2 mm of the alveolar labial bone wall, in accordance with Lopez-Jarana et al.'s study.[29] On the palatal aspect, previous studies showed that the palatal bone thickness was thick and increased apically,[7,30] comparable to the result of our study. According to the restorative-driven surgery concept, Wang et al.[31] suggested that the dental implant should mimic the natural tooth root in the contralateral and parallel to the tooth root axis. Additionally, Chung et al.[32] recommended that the implant should be placed to mimic the original root angulation but located more palatal due to the thicker palatal native bone. The results from our study assisted in planning following this concept.

In terms of SRP, the most prevalent root positions in the alveolar bone housing of maxillary central incisors in this study were classified as class I SRP (96.4%), followed by class II and class IV SRP. Class III SRP was not found within the dataset based on Kan et al.[5]. Additionally, our finding found a higher frequency of class I SRP. The result was in accordance with the previous studies on Thai and Asian populations. The prevalence of the buccal root position of the maxillary central incisor has been 92.2% to 95.4%[33,34], while class III SRP has been reported as the rarest of all classes.[8,35] Lombardo et al.[36] reported that the dental and alveolar arch forms differed in

width and depth in different ethnic groups. Therefore, the reason for the difference in SRP might be due to ethnic differences.

The result concerned the dental arch form, alveolar bone thickness, and SRP. There was no association between the dental arch form and SRP, while the alveolar bone thickness demonstrated the association with the dental arch form and SRP. This result supported that only the dental arch form could not be used to predict the SRP classification. Then, the relationship of the collected data in pairs was analyzed.

Regarding the association between alveolar bone thickness and dental arch form, alveolar bone thickness shows dissimilarity thickness on the labial aspect at mid-root and root apex level (Lm and La), palatal bone thickness at 3 mm apically from the CEJ (Pi), and palatal bone thickness at the root apex level (Pa). At the same time, there was no difference in the palatal bone thickness at the mid-root (Pm), labial bone thickness at 3 mm apically from the CEJ (Li), and alveolar bone thickness (LaPa) among the dental arch form.



The square dental arch form showed the highest alveolar bone thickness of the palatal aspect (Pa), while the labial aspect showed the thinnest bone thickness at the apex level (La). The taper arch showed the highest bone at the labial aspect (La) at the root apex level but less than 2 mm and showed the highest labial bone thickness at the mid root (Lm). The oval arch form, which was the most prevalent type, showed the lowest alveolar bone thickness of the

palatal aspect at the root apex level (Pa). Considering the arch form classification in this study, the less anterior cantilever in square dental arch form showed the lingual-inclined maxillary central incisors, reducing the labial bone thickness at the root apex level following the Tian et al.'s study.[30] On the other hand, the square arch form seemed more favorable for implant anchorage related to the immediate implant placement locations due to the greater palatal alveolar bone thickness. According to Kim et al.'s study[37], the implant was recommended parallel to the labial alveolar plate and slightly inclined more toward the labial than the incisal edge. Therefore, the taper arch form seemed to be suitable for this concept. However, types of the dental arch should be concerned to prevent the dental implant exposed to the labial wall in all arch types because all the dental arch forms have shown the alveolar bone thickness less than 2 mm of the labial aspect at the apex level.



In terms of alveolar bone thickness and SRP, class I SRP provided the highest bone thickness in the palatal aspect at all levels but showed the lowest bone thickness at the labial aspect at the mid-root and root apex level. Class II SRP showed the highest bone thickness in La, more than 2 mm. Class IV SRP showed the thinnest bone in the palatal aspect as the same result as the Khoury et al.[28] This information would help clinicians design the final implant position and angulation related to the alveolar bone thickness. Based on this study result, most root positions of maxillary central incisors were located buccally and demonstrated the high quantity of alveolar

bone at the palatal sites. As several studies reported, immediate implant placement should be placed in the palatal position parallel to the palatal plate to gain implant stability.[38] In class I SRP, the immediate implant position would be favorable to engage the apical and palatal bone and gain primary stability, which our study supported this concept. On the other hand, class II and IV SRP would allow the immediate implant position to follow the tooth socket, engaging the apical bone. This would leave more than 2 mm of labial bone at the implant apex.

In terms of age and sex difference, alveolar bone thickness in all measurement thickness areas showed statistically significant differences among groups. The alveolar bone thickness not more than 2 mm was shown along the labial aspect. All labial bone thickness showed the lowest bone thickness in the elderly female group. The elderly female group showed statistically significant differences in the alveolar bone thickness among groups and showed the lowest alveolar bone thickness on the palatal. Exceptionally the Pa showed the lowest thickness in the adult female group with no significant difference compared with the elderly female group. There were no statistical differences in males' age difference in all thicknesses. Gakonyo et al.[11] reported that the labial alveolar bone thickness decreased while aging. Our study showed different results in the male group but showed the difference in thickness in female groups. In contrast, a significant difference in alveolar bone thickness in female groups was found in Li, Lm,

La, and Pi. Following Zhang et al.[12], the labial bone was significantly thinner in postmenopausal women due to the increasing age and systemic condition.

Our result showed that increasing age solely has not resulted in reduced palatal bone thickness on the palatal aspect. At the root apex level and mid-root, the palatal bone thickness of adult females showed significant differences with both adult males and elderly males. In addition, the elderly male showed the same result. Similarly, Do et al.[6] presented that the palatal bone thickness at the apex level of the maxillary incisors differed significantly between the sexes. At 3 mm apically from CEJ, the palatal alveolar bone of elderly females showed the lowest bone thickness compared with male groups. LaPa showed significant differences in alveolar bone thickness between elderly females and both male groups, while no difference thickness from age difference. Soumya et al.[7] showed the significant influence of sex on the palatal alveolar bone thickness. These results suggested that clinicians should be aware of the minimal labial and palatal bone thickness in females, especially in elderly females.



Our study showed the correlation among the dental arch form, SRP, age-sex groups, and alveolar bone thickness. Consider the effect of dental arch form with the alveolar bone thickness at the apex level. Square arch form's patients showed a positive correlation in alveolar bone thickness at the apex level of the palatal aspect, while a negative correlation was shown at the apex level of the labial aspect. In the taper arch form's patients, a negative correlation was

shown only at the apex level of the palatal aspect. The dental arch form showed no correlation with the alveolar bone thickness at the mid-root area. Excluding the class I SRP, Class II and Class IV SRP showed a negative correlation between SRP classification and alveolar bone thickness, decreasing the alveolar bone thickness at the mid-root and apex level of the palatal aspect. Another factor that showed the negative effect on the alveolar bone thickness was age-sex groups. All-female groups had negative correlations at both palatal aspects, while the elderly female group had more negative correlations at the labial apex level than all other groups. This result agreed with the previous study, which showed the significantly higher bone volume in males than females at the apex and mid-root of maxillary central incisors.[7,8] In contrast, adult males and elderly males had no difference in correlation to bone thickness. Similar to the findings of Linjawi et al.[39], the result showed that age and sex-related had a negative effect on the anterior maxillary alveolar bone thickness at the apex level. Following the standardized coefficient (Beta), the elderly female shows the highest value that can affect the alveolar bone thickness. Considering that some studies found no correlation between elder and alveolar bone thickness, the combination of elder and female might prove significant. Systemic conditions and post-menstrual syndrome might be a factor in play for more bone resorption.



A common limitation of this study, in the retrospective study, was the various setting of the voxel size. The previous study showed that the 0.2-mm or 0.4-mm voxel delivered a similarly

accurate 3D CBCT model, and a larger voxel could reduce radiation exposure.[40] In fact, some image viewers could not reconstruct and measure the linear distance under the larger voxel size. The difference in voxel size might be problematic in measuring distance in some software. This factor was mitigated in the current study by utilizing an image viewer to interpret CBCT images in 1 mm intervals (slices). Further study would eliminate this factor entirely by specifying the voxel size used.

In summary, there were significant pairwise correlations. The dental arch form played an essential role in determining the alveolar bone thickness. According to the arch form classification in this study, the square arch form had the highest palatal bone thickness, while the labial bone in all arch types at the root apex level was thin. The dental arch form did not predict the SRP. Age and sex differences also influenced the alveolar bone thickness. The adult female negatively correlated to the alveolar bone thickness on the palatal aspect, while the elderly female showed a negative correlation at all sites. Therefore, the operator should consider the dental arch form, age-sex groups with great caution and inform the bone condition to the patients, especially in the elderly female patient. The bone volume prediction considering these factors could aid in planning immediate implant placement at the maxillary central incisor site. This data would result in a better aesthetic outcome and long-term success.

# REFERENCES

1. Fillion M, Aubazac D, Bessadet M, Allègre M, Nicolas E. The impact of implant treatment on oral health related quality of life in a private dental practice: a prospective cohort study. Health and quality of life outcomes. 2013;11(1):1-7.

2. Angkaew C, Serichetaphongse P, Krisdapong S, Dart MM, Pimkhaokham A. Oral health-related quality of life and esthetic outcome in single anterior maxillary implants. Clinical oral implants research. 2017;28(9):1089-96.

3. Morton D, Chen ST, Martin WC, Levine RA, Buser D. Consensus statements and recommended clinical procedures regarding optimizing esthetic outcomes in implant dentistry. The International journal of oral & maxillofacial implants. 2014;29:216-20.

4. Buser D, Martin W, Belser UC. Optimizing esthetics for implant restorations in the anterior maxilla: anatomic and surgical considerations. International Journal of Oral & Maxillofacial Implants. 2004;19(7).

5. Quirynen M, Van Assche N, Botticelli D, Berglundh T. How does the timing of implant placement to extraction affect outcome? Database of Abstracts of Reviews of Effects (DARE): Quality-assessed Reviews [Internet]. 2007.

6. Grunder U, Gracis S, Capelli M. Influence of the 3-D bone-to-implant relationship on esthetics. International Journal of Periodontics & Restorative Dentistry. 2005;25(2).

7. Kan JY, Roe P, Rungcharassaeng K, Patel RD, Waki T, Lozada JL, et al. Classification of sagittal root position in relation to the anterior maxillary osseous housing for immediate implant placement: a cone beam computed tomography study. International Journal of Oral & Maxillofacial Implants. 2011;26(4).

8. Kan JYK, Rungcharassaeng K, Deflorian M, Weinstein T, Wang HL, Testori T. Immediate implant placement and provisionalization of maxillary anterior single implants. Periodontology 2000. 2018;77(1):197-212.

9. Brügger OE, Bornstein MM, Kuchler U, Janner S, Chappuis V, Buser D. Implant therapy in a surgical specialty clinic: an analysis of patients, indications, surgical procedures, risk factors, and early failures. Int J Oral Maxillofac Implants. 2015;30(1):151-60.

10. Schimmel M, Müller F, Suter V, Buser D. Implants for elderly patients. Periodontology 2000. 2017;73(1):228-40.

11. Nations U. World Population Ageing 2019: Highlights (ST/ESA/SER.A/430). Department of Economic and Social Affairs, Population Division (2019) 2019.

12. Ikebe K, Wada M, Kagawa R, Maeda Y. Is old age a risk factor for dental implants? Japanese Dental Science Review. 2009;45(1):59-64.

13. Moy PK, Medina D, Shetty V, Aghaloo TL. Dental implant failure rates and associated risk factors. International Journal of Oral & Maxillofacial Implants. 2005;20(4).

14. Joseph Gakonyo B, Implantology P, Mohamedali AJ, Mungure EK. Cone beam computed tomography assessment of the buccal bone thickness in anterior maxillary teeth: relevance to immediate implant placement. The International journal of oral & maxillofacial implants. 2018;33(4).

15. Do TA, Shen YW, Fuh LJ, Huang HL. Clinical assessment of the palatal alveolar bone thickness and its correlation with the buccolingual angulation of maxillary incisors for immediate implant placement. Clinical implant dentistry and related research. 2019;21(5):1080-6.

16. Zhang CY, DeBaz C, Bhandal G, Alli F, Francisco MCB, Thacker HL, et al. Buccal bone thickness in the esthetic zone of postmenopausal women: A CBCT analysis. Implant dentistry. 2016;25(4):478-84.

17. Chan H-L, Misch K, Wang H-L. Dental imaging in implant treatment planning. Implant dentistry. 2010;19(4):288-98.

18. Bulyalert A, Pimkhaokham A. A novel classification of anterior alveolar arch forms and alveolar bone thickness: A cone-beam computed tomography study. Imaging science in dentistry. 2018;48(3):191-9.

19. Misch CE. Maxillary arch implant considerations: Fixes and overdenture prosthesis. Contemporary Implant Dentistry, ed. 2008;3:367-88.

20. Baumgaertel S, Palomo JM, Palomo L, Hans MG. Reliability and accuracy of cone-beam computed tomography dental measurements. American journal of orthodontics and dentofacial orthopedics. 2009;136(1):19-25.

21. Alam MK, Shahid F, Purmal K, Ahmad B, Khamis MF. Tooth size and dental arch dimension measurement through cone beam computed tomography: effect of age and

gender. Res J Recent Sci ISSN. 2014;2277:2502.

22. Chuck GC. Ideal arch form. The Angle Orthodontist. 1934;4(4):312-27.

23. Petaibunlue S, Serichetaphongse P, Pimkhaokham A. Influence of the anterior arch shape and root position on root angulation in the maxillary esthetic area. Imaging science in dentistry. 2019;49(2):123-30.

24. Sagat G, Yalcin S, Gultekin BA, Mijiritsky E. Influence of arch shape and implant position on stress distribution around implants supporting fixed full-arch prosthesis in edentulous maxilla. Implant dentistry. 2010;19(6):498-508.

25. Preti G, Pera P, Bassi F. Prediction of the shape and size of the maxillary anterior arch in edentulous patients. Journal of oral rehabilitation. 1986;13(2):115-25.

26. Misch CE. Maxillary arch implant considerations: Fixes and overdenture prosthesis. Contemporary Implant Dentistry, ed. 2007;3:367-88.

27. Al Shammout RW, Al Jabrah O, Aburumman K, Alhabahbah AM, Almanaseer W. The Effect of various classes of malocclusions on the maxillary arch forms and dimensions in Jordanian population. Adv Dent Oral Health. 2016;2:1-7.

28. Al-Zubair NM. Determinant factors of Yemeni maxillary arch dimensions. The Saudi dental journal. 2015;27(1):50-4.

29. Spray JR, Black CG, Morris HF, Ochi S. The influence of bone thickness on facial marginal bone response: stage 1 placement through stage 2 uncovering. Annals of Periodontology. 2000;5(1):119-28.

30. Wang H-m, Shen J-w, Yu M-f, Chen X-y, Jiang Q-h, He F-m. Analysis of facial bone wall dimensions and sagittal root position in the maxillary esthetic zone: a retrospective study using cone beam computed tomography. International Journal of Oral & Maxillofacial Implants. 2014;29(5).

31. Xu D, Wang Z, Sun L, Lin Z, Wan L, Li Y, et al. Classification of the root position of the maxillary central incisors and its clinical significance in immediate implant placement. Implant dentistry. 2016;25(4):520-4.

32. Jung Y-H, Cho B-H, Hwang JJ. Analysis of the root position of the maxillary incisors in the alveolar bone using cone-beam computed tomography. Imaging science in dentistry. 2017;47(3):181-7.

33. Giglou K, Batal H, Mehra P. Does Sagittal Root Position Affect Buccal or Palatal

Bone Thickness in the Anterior Esthetic Zone? Journal of Oral and Maxillofacial Surgery. 2017;75(10):e354-e5.

34. Petaibunlue S, Serichetaphongse P, Pimkhaokham A. Influence of the anterior arch shape and root position on root angulation in the maxillary esthetic area. Imaging science in dentistry. 2019;49(2):123.

35. Chen J, Ahmad R, Li W, Swain M, Li Q. Biomechanics of oral mucosa. Journal of the Royal Society Interface. 2015;12(109):20150325.

36. Tarnow D, Cho S, Wallace S. The effect of inter-implant distance on the height of inter-implant bone crest. Journal of periodontology. 2000;71(4):546-9.

37. Hermann JS, Cochran DL, Hermann JS, Buser D, Schenk RK, Schoolfield JD. Biologic Width around one-and two-piece titanium implants: A histometric evaluation of unloaded nonsubmerged and submerged implants in the canine mandible. Clinical oral implants research. 2001;12(6):559-71.

38. Jivraj S, Chee W. Treatment planning of implants in the aesthetic zone. British dental journal. 2006;201(2):77-89.

39. Romeo E, Chiapasco M, Ghisolfi M, Vogel G. Long-term clinical effectiveness of oral implants in the treatment of partial edentulism: Seven-year life table analysis of a prospective study with ITI® Dental Implants System used for single-tooth restorations. Clinical Oral Implants Research. 2002;13(2):133-43.

40. United Nations DoEaSA, Population Division (2019). World Population Ageing, (ST/ESA/SER.A/430). H. World Population Ageing. 2019.

41. DESA U. United Nations Department of Economic and Social Affairs/Population Division (2009b): World Population Prospects: The 2008 Revision. Internet: http://esa un org/unpp (gelesen am 16. 2010.

42. Nations U. World population prospects: the 2017 revision, key findings and advance tables. United Nations, New york. 2017.

43. He W, Goodkind D, Kowal PR. An aging world: 2015. 2016.

44. Shaw Jr RB, Kahn DM. Aging of the midface bony elements: a three-dimensional computed tomographic study. Plastic and reconstructive surgery. 2007;119(2):675-81.

45. Shaw Jr RB, Katzel EB, Koltz PF, Kahn DM, Puzas EJ, Langstein HN. Facial bone

density: effects of aging and impact on facial rejuvenation. Aesthetic surgery journal. 2012;32(8):937-42.

46. Flowers RS. Periorbital aesthetic surgery for men. Eyelids and related structures. Clinics in plastic surgery. 1991;18(4):689-729.

47. Mendelson B, Wong C-H. Changes in the facial skeleton with aging: implications and clinical applications in facial rejuvenation. Aesthetic plastic surgery. 2012;36(4):753-60.

48. Merheb J, Temmerman A, Coucke W, Rasmusson L, Kübler A, Thor A, et al. Relation between spongy bone density in the maxilla and skeletal bone density. Clinical implant dentistry and related research. 2015;17(6):1180-7.

49. Merheb J, Vercruyssen M, Coucke W, Quirynen M. Relationship of implant stability and bone density derived from computerized tomography images. Clinical implant dentistry and related research. 2018;20(1):50-7.

50. Chen LC, Lundgren T, Hallström H, Cherel F. Comparison of different methods of assessing alveolar ridge dimensions prior to dental implant placement. Journal of periodontology. 2008;79(3):401-5.

51. Mozzo P, Procacci C, Tacconi A, Martini PT, Andreis IB. A new volumetric CT machine for dental imaging based on the cone-beam technique: preliminary results. European radiology. 1998;8(9):1558-64.

52. Poeschl PW, Schmidt N, Guevara-Rojas G, Seemann R, Ewers R, Zipko HT, et al. Comparison of cone-beam and conventional multislice computed tomography for image-guided dental implant planning. Clinical oral investigations. 2013;17(1):317-24.

53. Ghassemian M, Nowzari H, Lajolo C, Verdugo F, Pirronti T, D'Addona A. The thickness of facial alveolar bone overlying healthy maxillary anterior teeth. Journal of periodontology. 2012;83(2):187-97.

54. Braut V, Bornstein MM, Belser U, Buser D. Thickness of the anterior maxillary facial bone wall—a retrospective radiographic study using cone beam computed tomography. International Journal of Periodontics and Restorative Dentistry. 2011;31(2):125.

55. Tyndall DA, Price JB, Tetradis S, Ganz SD, Hildebolt C, Scarfe WC. Position statement of the American Academy of Oral and Maxillofacial Radiology on selection

criteria for the use of radiology in dental implantology with emphasis on cone beam computed tomography. Oral surgery, oral medicine, oral pathology and oral radiology. 2012;113(6):817-26.

56. Spear F. Maintenance of the interdental papilla following anterior tooth removal. Practical periodontics and aesthetic dentistry: PPAD. 1999;11(1):21-8; quiz 30.

57. Saadoun A. The key to peri-implant esthetics: hard and soft tissue management. Dent Implantol Update. 1997;8:41-6.

58. Lee S-L, Kim H-J, Son M-K, Chung C-H. Anthropometric analysis of maxillary anterior buccal bone of Korean adults using cone-beam CT. The journal of advanced prosthodontics. 2010;2(3):92-6.

# APPENDIX

Data of Anterior maxillary dental arch form classification

| Case No. | Arch Type | Case No. | Arch Type | Case No. | Arch Type | Case No. | Arch Type | Case No. | Arch Type | Case No. | Arch Type | Case No. | Arch Type |
|---|---|---|---|---|---|---|---|---|---|---|---|---|---|
| 1 | O | 21 | T | 41 | S | 61 | O | 81 | O | 101 | T | 121 | O |
| 2 | S | 22 | O | 42 | O | 62 | O | 82 | O | 102 | T | 122 | S |
| 3 | T | 23 | O | 43 | S | 63 | O | 83 | O | 103 | O | 123 | T |
| 4 | O | 24 | S | 44 | O | 64 | O | 84 | T | 104 | O | 124 | O |
| 5 | T | 25 | O | 45 | O | 65 | S | 85 | O | 105 | S | 125 | S |
| 6 | T | 26 | O | 46 | O | 66 | O | 86 | O | 106 | T | 126 | O |
| 7 | S | 27 | O | 47 | O | 67 | O | 87 | O | 107 | O | 127 | O |
| 8 | O | 28 | O | 48 | O | 68 | O | 88 | O | 108 | O | 128 | T |
| 9 | S | 29 | T | 49 | O | 69 | T | 89 | O | 109 | O | 129 | S |
| 10 | S | 30 | S | 50 | O | 70 | T | 90 | O | 110 | S | 130 | O |
| 11 | S | 31 | O | 51 | T | 71 | S | 91 | O | 111 | O | 131 | T |
| 12 | S | 32 | O | 52 | S | 72 | O | 92 | O | 112 | O | 132 | O |
| 13 | S | 33 | O | 53 | O | 73 | O | 93 | O | 113 | S | 133 | O |
| 14 | S | 34 | S | 54 | S | 74 | O | 94 | S | 114 | T | 134 | O |
| 15 | O | 35 | T | 55 | O | 75 | O | 95 | O | 115 | T | 135 | S |
| 16 | S | 36 | S | 56 | O | 76 | O | 96 | O | 116 | T | 136 | S |
| 17 | O | 37 | S | 57 | O | 77 | O | 97 | T | 117 | O | 137 | S |
| 18 | S | 38 | O | 58 | O | 78 | T | 98 | O | 118 | O | 138 | O |
| 19 | S | 39 | O | 59 | T | 79 | T | 99 | O | 119 | S | 139 | O |
| 20 | O | 40 | O | 60 | O | 80 | O | 100 | O | 120 | S | 140 | T |

Data of Anterior maxillary dental arch form classification

| Case No. | Arch Type | Case No. | Arch Type | Case No. | Arch Type | Case No. | Arch Type | Case No. | Arch Type | Case No. | Arch Type | Case No. | Arch Type |
|---|---|---|---|---|---|---|---|---|---|---|---|---|---|
| 141 | S | 161 | T | 181 | T | 201 | O | 221 | S | 241 | O | 261 | S |
| 142 | O | 162 | S | 182 | O | 202 | O | 222 | S | 242 | T | 262 | T |
| 143 | S | 163 | O | 183 | O | 203 | O | 223 | O | 243 | O | 263 | T |
| 144 | O | 164 | O | 184 | T | 204 | T | 224 | S | 244 | O | 264 | S |
| 145 | O | 165 | T | 185 | O | 205 | S | 225 | T | 245 | T | 265 | O |
| 146 | T | 166 | T | 186 | S | 206 | S | 226 | O | 246 | S | 266 | S |
| 147 | O | 167 | S | 187 | O | 207 | O | 227 | O | 247 | O | 267 | S |
| 148 | S | 168 | O | 188 | O | 208 | O | 228 | T | 248 | O | 268 | S |
| 149 | O | 169 | O | 189 | O | 209 | S | 229 | O | 249 | T | 269 | S |
| 150 | S | 170 | O | 190 | T | 210 | T | 230 | S | 250 | O | 270 | O |
| 151 | O | 171 | O | 191 | S | 211 | S | 231 | T | 251 | T | 271 | T |
| 152 | S | 172 | S | 192 | T | 212 | T | 232 | S | 252 | O | 272 | T |
| 153 | T | 173 | O | 193 | S | 213 | T | 233 | O | 253 | S | 273 | S |
| 154 | S | 174 | T | 194 | O | 214 | O | 234 | T | 254 | T | 274 | T |
| 155 | O | 175 | S | 195 | S | 215 | T | 235 | O | 255 | T | 275 | T |
| 156 | O | 176 | O | 196 | O | 216 | S | 236 | S | 256 | S | 276 | T |
| 157 | T | 177 | T | 197 | S | 217 | T | 237 | S | 257 | O | 277 | O |
| 158 | O | 178 | O | 198 | S | 218 | O | 238 | T | 258 | S | 278 | S |
| 159 | S | 179 | T | 199 | O | 219 | T | 239 | O | 259 | T | 279 | S |
| 160 | O | 180 | T | 200 | S | 220 | T | 240 | S | 260 | S | 280 | S |

Data of Arch type S: Square arch form

| Case No. | 11_Li | 11_Pi | 11_Lm | 11_Pm | 11_La | 11_Pa | 11_LaPa | 11_SRP | 21_Li | 21_Pi | 21_Lm | 21_Pm | 21_La | 21_Pa | 21_LaPa | 21_SRP |
|---|---|---|---|---|---|---|---|---|---|---|---|---|---|---|---|---|
| 2 | 0 | 3 | 0 | 5 | 0.9 | 10 | 10.9 | 1 | 0 | 0.7 | 0 | 4.5 | 1 | 10.5 | 11.5 | 1 |
| 7 | 0 | 1 | 0 | 4.2 | 1.3 | 10.8 | 12.1 | 1 | 0 | 0.8 | 0.5 | 4.7 | 0.9 | 10.5 | 11.4 | 1 |
| 9 | 0 | 0.7 | 0 | 3.2 | 2.2 | 7.2 | 9.4 | 1 | 0 | 1.8 | 0 | 4.2 | 1.7 | 9.2 | 10.9 | 1 |
| 10 | 0 | 1.4 | 0.6 | 3.1 | 1.2 | 5 | 6.2 | 1 | 0 | 1.3 | 0.6 | 2.7 | 0.9 | 6.3 | 7.2 | 1 |
| 11 | 1.1 | 0.9 | 0.6 | 3.6 | 1.3 | 9.3 | 10.6 | 1 | 1.1 | 0.6 | 0.8 | 2.9 | 2 | 7.9 | 9.9 | 1 |
| 12 | 1.7 | 2.2 | 1 | 5.1 | 1.3 | 7.7 | 9 | 1 | 1.3 | 2 | 0.8 | 4.1 | 1.1 | 8.6 | 9.7 | 1 |
| 13 | 1.1 | 1.7 | 0.9 | 5.4 | 1.6 | 9.7 | 11.3 | 1 | 1.1 | 2.1 | 0.6 | 4.2 | 1.7 | 8.1 | 9.8 | 1 |
| 14 | 0.8 | 0.8 | 0.9 | 1.3 | 0.9 | 7 | 7.9 | 1 | 0.4 | 0.8 | 0.9 | 1.9 | 1 | 6.1 | 7.1 | 1 |
| 16 | 1.1 | 1.3 | 1.1 | 3.9 | 1.3 | 9.3 | 10.6 | 1 | 0 | 1.3 | 0.8 | 3.4 | 1.3 | 8.9 | 10.2 | 1 |
| 18 | 0.6 | 1.3 | 0.6 | 4 | 2.1 | 7.2 | 9.3 | 1 | 0.6 | 1.3 | 0.6 | 3.3 | 2.1 | 6.2 | 8.3 | 1 |
| 19 | 0.4 | 0.8 | 1 | 4.1 | 1 | 9.6 | 10.6 | 1 | 0 | 0.6 | 0.7 | 4.1 | 1.5 | 9 | 10.5 | 1 |
| 24 | 0.7 | 0.7 | 0.6 | 1.7 | 1.1 | 7 | 8.1 | 1 | 0.6 | 1.2 | 0.6 | 3.4 | 1.1 | 7.2 | 8.3 | 1 |
| 30 | 0.4 | 1.2 | 0.5 | 5.1 | 0.9 | 11 | 11.9 | 1 | 0.4 | 0.9 | 0.3 | 4.7 | 0.6 | 11.7 | 12.3 | 1 |
| 34 | 0.6 | 0.6 | 0.6 | 4.7 | 0.7 | 10.8 | 11.5 | 1 | 0.6 | 1.1 | 0.8 | 4.9 | 1.1 | 9.4 | 10.5 | 1 |
| 36 | 1.3 | 1.4 | 1 | 2.9 | 1.7 | 6.7 | 8.4 | 1 | 1 | 2.4 | 1 | 3.6 | 2.4 | 6.2 | 8.6 | 1 |
| 37 | 1.8 | 1.3 | 1.3 | 4.4 | 3 | 9.8 | 12.8 | 2 | 1.4 | 1.9 | 0.9 | 4.2 | 2.5 | 9.7 | 12.2 | 2 |
| 41 | 0.7 | 0.7 | 0.4 | 1.7 | 0.7 | 6.2 | 6.9 | 1 | 0.7 | 1 | 0.4 | 1.8 | 0.7 | 4.4 | 5.1 | 1 |
| 43 | 0.4 | 1.2 | 0.6 | 1.6 | 0.7 | 7.5 | 8.2 | 1 | 0.9 | 1 | 1 | 1.7 | 1.4 | 6.6 | 8 | 1 |

Data of Arch type S: Square arch form

| Case No. | 11_Li | 11_Pi | 11_Lm | 11_Pm | 11_La | 11_Pa | 11_LaPa | 11_SRP | 21_Li | 21_Pi | 21_Lm | 21_Pm | 21_La | 21_Pa | 21_LaPa | 21_SRP |
|---|---|---|---|---|---|---|---|---|---|---|---|---|---|---|---|---|
| 65 | 0.7 | 4 | 1.6 | 3.1 | 1.6 | 9.2 | 10.8 | 1 | 1.6 | 1.4 | 1.6 | 4 | 1.6 | 9.2 | 10.8 | 1 |
| 71 | 0.5 | 1.3 | 1.2 | 3.1 | 2.4 | 6.8 | 9.2 | 1 | 0.9 | 2.3 | 1.9 | 3.9 | 0.8 | 9 | 9.8 | 1 |
| 94 | 0.8 | 2.1 | 0.6 | 6.8 | 1.6 | 14.1 | 15.7 | 1 | 0.8 | 1.7 | 0.6 | 4.9 | 1.4 | 11.1 | 12.5 | 1 |
| 105 | 0.7 | 1.8 | 0.6 | 4.4 | 2 | 8.8 | 10.8 | 1 | 0.7 | 1.8 | 0.8 | 4.7 | 1.7 | 9.5 | 11.2 | 1 |
| 110 | 1 | 2.7 | 0.7 | 6.8 | 0.8 | 14.1 | 14.9 | 1 | 0.9 | 3.5 | 0.7 | 6.8 | 1.3 | 12.9 | 14.2 | 1 |
| 113 | 0.9 | 1.4 | 0.5 | 5.4 | 0.6 | 10.4 | 11 | 1 | 0.7 | 1.4 | 0.7 | 4.5 | 1.4 | 9.2 | 10.6 | 1 |
| 119 | 1 | 1.7 | 1.2 | 4.2 | 2.1 | 7.7 | 9.8 | 1 | 0.6 | 0.8 | 0.9 | 3.8 | 2.1 | 8.4 | 10.5 | 1 |
| 120 | 0 | 1 | 0.7 | 2.7 | 1.1 | 7.4 | 8.5 | 1 | 0 | 1.1 | 0.8 | 3.3 | 1.1 | 8.2 | 9.3 | 1 |
| 122 | 1.6 | 1.7 | 1.8 | 3.7 | 1.4 | 5.7 | 7.1 | 1 | 1.5 | 1.8 | 0.9 | 4.3 | 1.2 | 7.2 | 8.4 | 1 |
| 125 | 0.9 | 0.6 | 0.5 | 2.9 | 0.5 | 7.9 | 8.4 | 1 | 0.7 | 0.8 | 0.7 | 3.2 | 0.5 | 8.7 | 9.2 | 1 |
| 129 | 0.6 | 1.8 | 0.6 | 4.5 | 0.6 | 10.6 | 11.2 | 1 | 0.6 | 2.1 | 0.6 | 5.4 | 0.6 | 11.5 | 12.1 | 1 |
| 135 | 0 | 2.8 | 0.8 | 5.9 | 0.8 | 12.1 | 12.9 | 1 | 0 | 1.6 | 0.8 | 3.3 | 0.8 | 11.5 | 12.3 | 1 |
| 136 | 1.2 | 1.1 | 1.1 | 3 | 2.3 | 8 | 10.3 | 1 | 1.3 | 1.1 | 1 | 3 | 2.3 | 7.8 | 10.1 | 1 |
| 137 | 1.8 | 1.1 | 0.5 | 4.8 | 1.2 | 9.6 | 10.8 | 1 | 1.4 | 1.3 | 0.5 | 4.9 | 1.8 | 9.6 | 11.4 | 1 |
| 141 | 0.7 | 1 | 1.1 | 2.8 | 3 | 7.7 | 10.7 | 1 | 0.7 | 1 | 0.7 | 2.8 | 1.5 | 8.8 | 10.3 | 1 |
| 143 | 1 | 0.6 | 0.7 | 3.3 | 1.8 | 7.6 | 9.4 | 1 | 1.3 | 0.8 | 0.7 | 2.1 | 0.8 | 7.9 | 8.7 | 1 |
| 148 | 2.2 | 2.3 | 0.8 | 2.9 | 2.9 | 7.4 | 10.3 | 1 | 1.3 | 2.3 | 0.8 | 2.9 | 2.9 | 7.4 | 10.3 | 1 |
| 150 | 0.6 | 2 | 1.2 | 6.8 | 2.7 | 10.8 | 13.5 | 1 | 1.1 | 1.9 | 0.7 | 4.8 | 1.7 | 10.7 | 12.4 | 1 |

Data of Arch type S: Square arch form

| Case No. | 11_Li | 11_Pi | 11_Lm | 11_Pm | 11_La | 11_Pa | 11_LaPa | 11_SRP | 21_Li | 21_Pi | 21_Lm | 21_Pm | 21_La | 21_Pa | 21_LaPa | 21_SRP |
|---|---|---|---|---|---|---|---|---|---|---|---|---|---|---|---|---|
| 159 | 0 | 0 | 1.4 | 3.3 | 1.4 | 11.3 | 12.7 | 1 | 0 | 0 | 1.5 | 2.8 | 1.4 | 10.3 | 11.7 | 1 |
| 162 | 0.8 | 0.9 | 1.7 | 3.3 | 1.2 | 7.7 | 8.9 | 1 | 0.8 | 1.9 | 0.7 | 3.7 | 1.9 | 9.1 | 11 | 1 |
| 167 | 0.7 | 1.2 | 0.4 | 2.9 | 1.3 | 6.3 | 7.6 | 1 | 0.8 | 1.2 | 3.5 | 3.5 | 1.3 | 6.8 | 8.1 | 1 |
| 172 | 2.9 | 4 | 1.9 | 5.6 | 2.7 | 10.4 | 13.1 | 1 | 1.7 | 3 | 1.1 | 6 | 1.6 | 10.1 | 11.7 | 1 |
| 175 | 0.6 | 2 | 0.8 | 3.1 | 1.9 | 6.3 | 8.2 | 1 | 1.4 | 3 | 1.1 | 3.9 | 1.6 | 6 | 7.6 | 1 |
| 186 | 1 | 1.3 | 0.9 | 4.4 | 1.6 | 9.5 | 11.1 | 1 | 0.8 | 1.3 | 1 | 3.8 | 1.6 | 8.5 | 10.1 | 1 |
| 191 | 0 | 1 | 0.3 | 1.7 | 2.7 | 8.1 | 10.8 | 1 | 1.4 | 1.5 | 0.8 | 3.1 | 1.9 | 8.9 | 10.8 | 1 |
| 193 | 0.7 | 1.6 | 0.9 | 2 | 3.4 | 4.6 | 8 | 1 | 0.8 | 1.6 | 0.8 | 3.5 | 2.8 | 6.7 | 9.5 | 1 |
| 195 | 0 | 0.5 | 1.1 | 5.3 | 3.3 | 10.3 | 13.6 | 1 | 0 | 1.1 | 0.6 | 5 | 2.5 | 9.5 | 12 | 1 |
| 197 | 1.4 | 1 | 0.5 | 5.3 | 1.5 | 11 | 12.5 | 1 | 0.9 | 1.8 | 0.9 | 5.3 | 1.5 | 10 | 11.5 | 1 |
| 198 | 0.8 | 2.3 | 1.2 | 7 | 0.9 | 14.4 | 15.3 | 1 | 1 | 1.6 | 1.4 | 7.7 | 0.9 | 15.4 | 16.3 | 1 |
| 200 | 0.4 | 1.6 | 1.2 | 3.1 | 2.1 | 10.5 | 12.6 | 1 | 0.5 | 1.7 | 0.9 | 3.1 | 1.1 | 8.9 | 10 | 1 |
| 205 | 0.3 | 2.3 | 0.3 | 7.5 | 3 | 14.8 | 17.8 | 1 | 0.3 | 1.5 | 0.3 | 7.7 | 2.2 | 14.8 | 17 | 1 |
| 206 | 0.6 | 1.4 | 0.5 | 6.2 | 0.9 | 12.4 | 13.3 | 1 | 0.5 | 0.9 | 0.8 | 6 | 1.4 | 10.7 | 12.1 | 1 |
| 209 | 1 | 1.7 | 0.7 | 5.8 | 2.5 | 10.5 | 13 | 1 | 0.7 | 1.6 | 0.8 | 5.2 | 1.6 | 10.8 | 12.4 | 1 |
| 211 | 0.7 | 1.4 | 0.8 | 4 | 2 | 7.9 | 9.9 | 1 | 0.7 | 1.4 | 0.7 | 3.3 | 1.5 | 6.9 | 8.4 | 1 |
| 216 | 1.8 | 2.2 | 0.9 | 5.4 | 1.5 | 8.4 | 9.9 | 1 | 1.3 | 2.2 | 0.9 | 4.9 | 1.5 | 8.2 | 9.7 | 1 |
| 221 | 1.5 | 1.2 | 0.6 | 0.9 | 1.6 | 5.7 | 7.3 | 1 | 1.1 | 0.9 | 0.6 | 2.3 | 1.1 | 6.4 | 7.5 | 1 |

Data of Arch type S: Square arch form

| Case No. | 11_Li | 11_Pi | 11_Lm | 11_Pm | 11_La | 11_Pa | 11_LaPa | 11_SRP | 21_Li | 21_Pi | 21_Lm | 21_Pm | 21_La | 21_Pa | 21_LaPa | 21_SRP |
|---|---|---|---|---|---|---|---|---|---|---|---|---|---|---|---|---|
| 230 | 1.1 | 1.4 | 0.5 | 8.2 | 1 | 14.9 | 15.9 | 1 | 0.6 | 1.1 | 0.4 | 6.7 | 0.8 | 13.9 | 14.7 | 1 |
| 232 | 1.3 | 1.8 | 0.6 | 5.1 | 0.6 | 12.2 | 12.8 | 1 | 1.3 | 2.5 | 0.9 | 5.1 | 0.6 | 12.6 | 13.2 | 1 |
| 236 | 0.7 | 1.6 | 1.2 | 2.7 | 2.8 | 4.4 | 7.2 | 1 | 0.9 | 0.7 | 0.5 | 1.5 | 2.2 | 5.1 | 7.3 | 1 |
| 237 | 0.6 | 0.5 | 1.4 | 3.5 | 1.5 | 7.1 | 8.6 | 1 | 0.6 | 1.5 | 0.6 | 4.9 | 1.3 | 8.6 | 9.9 | 1 |
| 240 | 0.4 | 1.5 | 0.6 | 6.7 | 0.8 | 12.9 | 13.7 | 1 | 0.9 | 1.9 | 1.2 | 4 | 2.3 | 10.5 | 12.8 | 1 |
| 246 | 0.9 | 0.3 | 1.6 | 3.7 | 1.5 | 11 | 12.5 | 1 | 1 | 1.2 | 1.6 | 4.8 | 0.4 | 11.4 | 11.8 | 1 |
| 253 | 1.1 | 1.4 | 1.4 | 3.5 | 2.1 | 8.5 | 10.6 | 1 | 1.1 | 1.6 | 0.8 | 3.8 | 2.7 | 7.5 | 10.2 | 1 |
| 256 | 0.8 | 0 | 0.5 | 2.5 | 2 | 6.6 | 8.6 | 1 | 0 | 0 | 1.3 | 0.5 | 3 | 2.6 | 5.6 | 4 |
| 258 | 0.9 | 1 | 0.4 | 3.4 | 1.1 | 7 | 8.1 | 1 | 0.8 | 1.7 | 0.7 | 3.8 | 1.9 | 7.5 | 9.4 | 1 |
| 260 | 0.6 | 2.7 | 0.6 | 5.7 | 1.3 | 9.6 | 10.9 | 1 | 0.5 | 1.6 | 0.2 | 5.6 | 1.3 | 8.7 | 10 | 1 |
| 261 | 0.5 | 0 | 0.7 | 2.8 | 0.6 | 9.6 | 10.2 | 1 | 0 | 0 | 0.8 | 2.2 | 0.9 | 9.1 | 10 | 1 |
| 264 | 0.7 | 1.1 | 0.7 | 4.1 | 0.7 | 9 | 9.7 | 1 | 0 | 0 | 0.7 | 3.4 | 0.7 | 8.9 | 9.6 | 1 |
| 266 | 1.6 | 1 | 1.7 | 3.9 | 0.8 | 7.2 | 8 | 1 | 1 | 0.8 | 1 | 2.5 | 1.4 | 7.3 | 8.7 | 1 |
| 267 | 0.6 | 0.6 | 1.6 | 3.7 | 2.4 | 9.7 | 12.1 | 1 | 0 | 1.6 | 0.6 | 4.9 | 1.7 | 4.2 | 5.9 | 1 |
| 268 | 1.8 | 1.7 | 1.4 | 4.6 | 2.6 | 9.2 | 11.8 | 1 | 2.1 | 1.3 | 1.7 | 4.2 | 2.1 | 8.8 | 10.9 | 1 |
| 269 | 0.7 | 1.8 | 0.5 | 5.5 | 1.1 | 10.6 | 11.7 | 1 | 0.6 | 1.8 | 0.3 | 5.8 | 1.2 | 10.1 | 11.3 | 1 |
| 273 | 0 | 0.8 | 0.9 | 3.3 | 1 | 5.2 | 6.2 | 1 | 0 | 0.6 | 0.8 | 3.3 | 0.9 | 7.5 | 8.4 | 1 |
| 278 | 1.4 | 2.2 | 0.6 | 5.2 | 2.6 | 8.6 | 11.2 | 1 | 1.1 | 1.4 | 0.8 | 4.2 | 1.9 | 8.3 | 10.2 | 1 |

Data of Arch type O : Oval arch form

| Case No. | 11_Li | 11_Pi | 11_Lm | 11_Pm | 11_La | 11_Pa | 11_LaPa | 11_SRP | 21_Li | 21_Pi | 21_Lm | 21_Pm | 21_La | 21_Pa | 21_LaPa | 21_SRP |
|---|---|---|---|---|---|---|---|---|---|---|---|---|---|---|---|---|
| 1 | 1.4 | 2.4 | 1.1 | 5.5 | 1.3 | 10 | 11.3 | 1 | 0.9 | 2.9 | 0.8 | 5.4 | 1.3 | 11.5 | 12.8 | 1 |
| 4 | 1.2 | 1.7 | 0.6 | 3.8 | 1.4 | 8 | 9.4 | 1 | 1.6 | 1.6 | 1 | 2.6 | 1.6 | 6.8 | 8.4 | 1 |
| 8 | 0.7 | 1.5 | 0.9 | 6.3 | 1.2 | 11.3 | 12.5 | 1 | 1.7 | 0.6 | 1.1 | 3.4 | 1.8 | 6.3 | 8.1 | 1 |
| 15 | 0.6 | 2.1 | 0.6 | 4.7 | 1.8 | 8.4 | 10.2 | 1 | 0.7 | 1.9 | 0.7 | 4.8 | 1.9 | 7.9 | 9.8 | 1 |
| 17 | 0.7 | 1.8 | 1.5 | 2.9 | 2.8 | 5.9 | 8.7 | 1 | 0.6 | 1.4 | 0.7 | 2.5 | 2.6 | 5.5 | 8.1 | 1 |
| 20 | 0.6 | 1.4 | 0.3 | 5.1 | 1.5 | 10 | 11.5 | 1 | 0.4 | 0.9 | 0.3 | 3.8 | 1.2 | 7.9 | 9.1 | 1 |
| 22 | 1 | 1.2 | 0.5 | 3 | 2 | 6.6 | 8.6 | 1 | 1.3 | 1.1 | 0.5 | 2.6 | 1.5 | 6.4 | 7.9 | 1 |
| 23 | 1 | 1.8 | 1 | 4.1 | 3.4 | 8.1 | 11.5 | 1 | 1.3 | 1.4 | 1.3 | 3.7 | 2.7 | 7.6 | 10.3 | 1 |
| 25 | 0.5 | 1 | 0.7 | 3.6 | 2.2 | 8.1 | 10.3 | 1 | 0 | 1 | 1.6 | 3.6 | 1.3 | 8.1 | 9.4 | 1 |
| 26 | 0.9 | 1 | 0.4 | 2.1 | 1.8 | 6 | 7.8 | 1 | 0.3 | 0.5 | 0.9 | 1.4 | 2.5 | 5.7 | 8.2 | 1 |
| 27 | 0.7 | 1.4 | 0.6 | 3 | 2.3 | 7.7 | 10 | 1 | 0.7 | 2.2 | 0.5 | 3.8 | 2.3 | 7.2 | 9.5 | 1 |
| 28 | 1.1 | 1.5 | 1 | 8.1 | 1.4 | 13.7 | 15.1 | 1 | 0.7 | 1.1 | 0.5 | 8.2 | 1.3 | 13.5 | 14.8 | 1 |
| 31 | 0.6 | 1 | 1.6 | 2.4 | 2.7 | 6.3 | 9 | 1 | 0.6 | 1.3 | 1.5 | 3.5 | 2.7 | 7 | 9.7 | 1 |
| 32 | 0.4 | 1.1 | 0.2 | 1.5 | 1.2 | 4 | 5.2 | 1 | 0.3 | 1.1 | 0.5 | 1.8 | 2.2 | 4 | 6.2 | 1 |
| 33 | 1.8 | 1.6 | 0.6 | 2.7 | 0.7 | 6.1 | 6.8 | 1 | 1.1 | 1.4 | 0.6 | 2.8 | 0.7 | 5.9 | 6.6 | 1 |
| 38 | 1.2 | 1.7 | 0.8 | 3.5 | 2 | 7.2 | 9.2 | 1 | 1.2 | 1.7 | 0.5 | 3.8 | 1.8 | 7.3 | 9.1 | 1 |
| 39 | 0.3 | 1.8 | 0.7 | 4.6 | 2.8 | 8 | 10.8 | 1 | 0.3 | 1.8 | 0.7 | 2.5 | 2.1 | 5.9 | 8 | 1 |
| 40 | 0.9 | 1.3 | 0.6 | 3 | 1 | 9.3 | 10.3 | 1 | 1.1 | 1.3 | 0.6 | 3.8 | 0.6 | 10.2 | 10.8 | 1 |

Data of Arch type O : Oval arch form

| Case No. | 11_Li | 11_Pi | 11_Lm | 11_Pm | 11_La | 11_Pa | 11_LaPa | 11_SRP | 21_Li | 21_Pi | 21_Lm | 21_Pm | 21_La | 21_Pa | 21_LaPa | 21_SRP |
|---|---|---|---|---|---|---|---|---|---|---|---|---|---|---|---|---|
| 45 | 0.9 | 0.8 | 0.5 | 5.3 | 2.7 | 10.2 | 12.9 | 1 | 0 | 1.2 | 0.9 | 3.9 | 1.7 | 8.4 | 10.1 | 1 |
| 46 | 0.4 | 0 | 0.4 | 7.2 | 3.1 | 12.2 | 15.3 | 1 | 0.5 | 1.7 | 0.6 | 4.9 | 3.9 | 10.6 | 14.5 | 1 |
| 47 | 1.3 | 2.8 | 0.3 | 7.7 | 0.4 | 14.3 | 14.7 | 1 | 1.1 | 1.7 | 1 | 8 | 0.7 | 14 | 14.7 | 1 |
| 48 | 0.9 | 0.8 | 0.4 | 1.4 | 1.4 | 5.8 | 7.2 | 1 | 0.5 | 0.9 | 0.4 | 1 | 1.6 | 5.2 | 6.8 | 1 |
| 49 | 1.3 | 2.4 | 0.4 | 5.6 | 0.6 | 10.5 | 11.1 | 1 | 1.2 | 2.6 | 0.6 | 6.2 | 0.7 | 10.8 | 11.5 | 1 |
| 50 | 1.1 | 1.7 | 1.2 | 4.6 | 2.3 | 8.2 | 10.5 | 1 | 0.8 | 1.6 | 0.7 | 5 | 2.1 | 8.2 | 10.3 | 1 |
| 53 | 1.8 | 1.8 | 1.3 | 3.8 | 3 | 7.2 | 10.2 | 1 | 1.8 | 2.7 | 1.3 | 3.4 | 3 | 7.9 | 10.9 | 1 |
| 55 | 0.5 | 0 | 0.6 | 5 | 3.2 | 12.1 | 15.3 | 1 | 0.5 | 0.4 | 0.6 | 2.3 | 2 | 7.4 | 9.4 | 1 |
| 56 | 1 | 1.2 | 0.9 | 1 | 1.1 | 6.9 | 8 | 1 | 1.7 | 1.2 | 0.6 | 2.6 | 0.6 | 8.2 | 8.8 | 1 |
| 57 | 0.9 | 0.9 | 1.1 | 2.5 | 2.7 | 7.1 | 9.8 | 1 | 0.5 | 0.4 | 1 | 2 | 3.8 | 5.3 | 9.1 | 2 |
| 58 | 0.4 | 2.5 | 0.4 | 4.1 | 2.3 | 6.9 | 9.2 | 1 | 0.5 | 2.2 | 0.6 | 3.2 | 1.4 | 6.4 | 7.8 | 1 |
| 60 | 0 | 1.2 | 1.4 | 4.5 | 1.4 | 11 | 12.4 | 1 | 0 | 1.8 | 0.9 | 4.1 | 1.6 | 9.9 | 11.5 | 1 |
| 61 | 0.7 | 1.4 | 0.7 | 2.8 | 2.1 | 6.1 | 8.2 | 1 | 1.1 | 1.7 | 0.4 | 3.5 | 1.2 | 6.3 | 7.5 | 1 |
| 62 | 0.9 | 0.7 | 0.7 | 2.1 | 1 | 6.3 | 7.3 | 1 | 0.7 | 0.7 | 0.7 | 1.8 | 1.2 | 5.8 | 7 | 1 |
| 63 | 0.5 | 1.3 | 0.4 | 5.2 | 1.6 | 9.3 | 10.9 | 1 | 0.5 | 1.9 | 0.8 | 4.9 | 1.6 | 10.3 | 11.9 | 1 |
| 64 | 0.7 | 1.3 | 0.6 | 3.3 | 2.3 | 5.4 | 7.7 | 1 | 0.4 | 1.9 | 1.3 | 3.1 | 1.9 | 5.7 | 7.6 | 1 |
| 66 | 1.7 | 2 | 0.9 | 3.1 | 2.3 | 5.5 | 7.8 | 1 | 1.7 | 2.3 | 0.8 | 3.3 | 1.7 | 6 | 7.7 | 1 |
| 67 | 0.7 | 3.1 | 0.8 | 8 | 2.2 | 13.5 | 15.7 | 1 | 1.3 | 2.4 | 0.5 | 6.1 | 1.5 | 10.3 | 11.8 | 1 |

Data of Arch type O : Oval arch form

| Case No. | 11_Li | 11_Pi | 11_Lm | 11_Pm | 11_La | 11_Pa | 11_LaPa | 11_SRP | 21_Li | 21_Pi | 21_Lm | 21_Pm | 21_La | 21_Pa | 21_LaPa | 21_SRP |
|---|---|---|---|---|---|---|---|---|---|---|---|---|---|---|---|---|
| 73 | 0.7 | 1.5 | 0.7 | 4.6 | 0.9 | 9.6 | 10.5 | 1 | 0.6 | 1.3 | 0.7 | 5.8 | 1 | 10.4 | 11.4 | 1 |
| 74 | 0.7 | 2 | 0.4 | 3.4 | 6 | 6 | 12 | 1 | 0.4 | 1.3 | 0.7 | 4 | 2.4 | 6.3 | 8.7 | 1 |
| 75 | 0.9 | 0.5 | 0.6 | 2.4 | 1.2 | 6.1 | 7.3 | 1 | 1.2 | 1.1 | 0.7 | 3 | 1.2 | 6.3 | 7.5 | 1 |
| 76 | 0.6 | 2.8 | 0.8 | 4.8 | 0.9 | 8.5 | 9.4 | 1 | 0.8 | 1.5 | 1.1 | 3.4 | 1.4 | 7.4 | 8.8 | 1 |
| 77 | 1.2 | 0.7 | 1.1 | 4.5 | 1.6 | 9.6 | 11.2 | 1 | 1.1 | 1 | 1.3 | 3.5 | 2.4 | 9.2 | 11.6 | 1 |
| 80 | 0.5 | 1.3 | 0.8 | 4.3 | 1.1 | 12 | 13.1 | 1 | 0.9 | 2.2 | 0.8 | 5.4 | 0.6 | 10.6 | 11.2 | 1 |
| 81 | 0.7 | 0.6 | 0.4 | 1.2 | 2.4 | 4.4 | 6.8 | 1 | 0.7 | 1.6 | 0.8 | 3 | 1.7 | 5.3 | 7 | 1 |
| 82 | 0.6 | 1.6 | 0.6 | 4.4 | 1.3 | 9.3 | 10.6 | 1 | 0.9 | 1.6 | 0.7 | 3.2 | 1 | 7.9 | 8.9 | 1 |
| 83 | 1.5 | 1.1 | 1.4 | 4.9 | 3.7 | 9.9 | 13.6 | 1 | 0.7 | 0.8 | 1.5 | 4.9 | 4.3 | 9.2 | 13.5 | 1 |
| 85 | 1 | 1.4 | 0.6 | 2.9 | 2.6 | 9 | 11.6 | 1 | 1.5 | 2.4 | 0.7 | 4.8 | 1.8 | 9 | 10.8 | 1 |
| 86 | 0.9 | 2.8 | 0.6 | 6.4 | 1.5 | 10.1 | 11.6 | 1 | 0.6 | 2.8 | 0.7 | 4.2 | 1.5 | 8.5 | 10 | 1 |
| 87 | 0.9 | 2.1 | 0.6 | 5.3 | 1.5 | 10.3 | 11.8 | 1 | 0.9 | 2.1 | 0.7 | 6 | 1.5 | 9.2 | 10.7 | 1 |
| 88 | 2.1 | 0.5 | 1.2 | 2.1 | 1.7 | 4.7 | 6.4 | 1 | 1.1 | 0.9 | 0.5 | 3.3 | 0.5 | 8.2 | 8.7 | 1 |
| 89 | 0.6 | 1.2 | 0.8 | 2.2 | 4 | 6.4 | 10.4 | 1 | 0.6 | 1.5 | 0.9 | 2.8 | 2.3 | 6.8 | 9.1 | 1 |
| 90 | 1 | 0.9 | 0.6 | 2.6 | 0.9 | 6.8 | 7.7 | 1 | 0.9 | 2.1 | 0.6 | 3 | 0.4 | 5.8 | 6.2 | 1 |
| 91 | 0.5 | 0.9 | 1.4 | 4.2 | 2 | 11.8 | 13.8 | 1 | 0.7 | 0.9 | 0.9 | 4.2 | 0.8 | 12.9 | 13.7 | 1 |
| 92 | 0.9 | 1.3 | 0.4 | 4.4 | 1.5 | 9.7 | 11.2 | 1 | 0.9 | 1.9 | 0.6 | 5.4 | 1 | 9.9 | 10.9 | 1 |
| 93 | 0.6 | 1.6 | 0.5 | 3.3 | 1.3 | 7.1 | 8.4 | 1 | 1 | 1.6 | 0.7 | 3.9 | 1.2 | 8 | 9.2 | 1 |

Data of Arch type O : Oval arch form

| Case No. | 11_Li | 11_Pi | 11_Lm | 11_Pm | 11_La | 11_Pa | 11_LaPa | 11_SRP | 21_Li | 21_Pi | 21_Lm | 21_Pm | 21_La | 21_Pa | 21_LaPa | 21_SRP |
|---|---|---|---|---|---|---|---|---|---|---|---|---|---|---|---|---|
| 98 | 0.9 | 2.8 | 0.8 | 5.3 | 0.9 | 8.7 | 9.6 | 1 | 0.7 | 1.4 | 1 | 4.7 | 2 | 7.5 | 9.5 | 1 |
| 99 | 2 | 2.8 | 0.4 | 6 | 0.9 | 10.1 | 11 | 1 | 1.8 | 2.3 | 0.8 | 5.8 | 1.3 | 10.3 | 11.6 | 1 |
| 100 | 1.3 | 0.9 | 1.3 | 2.3 | 2 | 6.8 | 8.8 | 1 | 1.3 | 0.9 | 1.1 | 3.1 | 1.8 | 7 | 8.8 | 1 |
| 103 | 0.5 | 0.9 | 0.7 | 3.5 | 2.2 | 7.9 | 10.1 | 1 | 0.4 | 1.5 | 0.6 | 5.1 | 2 | 9.8 | 11.8 | 1 |
| 104 | 0.7 | 1.2 | 0.6 | 3.3 | 0.5 | 9.3 | 9.8 | 1 | 1 | 1.7 | 0.9 | 3.8 | 0.7 | 6.8 | 7.5 | 1 |
| 107 | 0.9 | 2.6 | 0.7 | 6.2 | 2.3 | 10.3 | 12.6 | 1 | 1.2 | 2.6 | 1 | 6.1 | 2.3 | 10.9 | 13.2 | 1 |
| 108 | 0.8 | 1.9 | 1.5 | 4.2 | 1.5 | 8 | 9.5 | 1 | 1.1 | 1.8 | 1.1 | 3.6 | 1.1 | 8.3 | 9.4 | 1 |
| 109 | 0.7 | 0.9 | 1 | 2 | 3 | 4.1 | 7.1 | 2 | 1.1 | 0.7 | 1 | 2 | 2 | 5.5 | 7.5 | 2 |
| 111 | 1.3 | 1.7 | 1 | 3.3 | 2.2 | 7.2 | 9.4 | 1 | 0.7 | 2.5 | 0.7 | 4.2 | 1.8 | 8.1 | 9.9 | 1 |
| 112 | 1.5 | 1.8 | 0.4 | 3.7 | 1.3 | 7.9 | 9.2 | 1 | 1.2 | 1.3 | 0.4 | 3.1 | 0.8 | 7 | 7.8 | 1 |
| 117 | 0.5 | 0.6 | 0.4 | 2.3 | 1.3 | 8.9 | 10.2 | 1 | 0 | 0 | 0.6 | 3.1 | 1.1 | 9 | 10.1 | 1 |
| 118 | 0 | 0 | 1 | 2.3 | 2 | 7.2 | 9.2 | 1 | 0 | 0.9 | 0.6 | 4.1 | 1.8 | 8.3 | 10.1 | 1 |
| 121 | 0.5 | 1.7 | 0.4 | 3.5 | 0.8 | 8.9 | 9.7 | 1 | 0.8 | 1.1 | 0.5 | 3.3 | 0.9 | 7.5 | 8.4 | 1 |
| 124 | 1.2 | 2.8 | 0.8 | 5.8 | 1.9 | 6.8 | 8.7 | 1 | 1.5 | 2.6 | 0.9 | 5.8 | 1.5 | 8 | 9.5 | 1 |
| 126 | 1.1 | 1.4 | 0.5 | 3.5 | 2.2 | 6.4 | 8.6 | 1 | 1.2 | 1.3 | 1 | 3.4 | 2.1 | 7.5 | 9.6 | 1 |
| 127 | 1.1 | 1.4 | 0.9 | 4.6 | 1.7 | 8.1 | 9.8 | 1 | 0.9 | 1.6 | 1.1 | 4.6 | 1.7 | 7.5 | 9.2 | 1 |
| 130 | 0 | 1.3 | 1.1 | 3.3 | 2.3 | 6.8 | 9.1 | 1 | 1.1 | 1.8 | 1.4 | 4.1 | 2.2 | 6.9 | 9.1 | 1 |
| 132 | 1.3 | 1.7 | 0.6 | 3.1 | 2 | 7.4 | 9.4 | 1 | 1.4 | 1.6 | 1 | 2.6 | 1.3 | 6.5 | 7.8 | 1 |

Data of Arch type O : Oval arch form

| Case No. | 11_Li | 11_Pi | 11_Lm | 11_Pm | 11_La | 11_Pa | 11_LaPa | 11_SRP | 21_Li | 21_Pi | 21_Lm | 21_Pm | 21_La | 21_Pa | 21_LaPa | 21_SRP |
|---|---|---|---|---|---|---|---|---|---|---|---|---|---|---|---|---|
| 229 | 1.5 | 1 | 1.1 | 2.8 | 2.2 | 6.1 | 8.3 | 1 | 1 | 1.4 | 0.9 | 3.1 | 2.2 | 6.2 | 8.4 | 1 |
| 233 | 0.7 | 2.7 | 1.4 | 4.5 | 2.7 | 7.7 | 10.4 | 1 | 0.8 | 2.1 | 0.9 | 4.5 | 1.8 | 8.3 | 10.1 | 1 |
| 235 | 2 | 2.2 | 1.4 | 6.7 | 2 | 11.5 | 13.5 | 1 | 1.1 | 2.8 | 0.6 | 6.2 | 2.9 | 9.7 | 12.6 | 1 |
| 239 | 0 | 1.4 | 1.1 | 2.6 | 2.9 | 7.1 | 10 | 1 | 0 | 0 | 0.9 | 2.6 | 2.5 | 7 | 9.5 | 1 |
| 241 | 0.5 | 3.1 | 0.5 | 6.1 | 1.2 | 11 | 12.2 | 1 | 0.6 | 2.2 | 0.3 | 6.4 | 2.1 | 10.5 | 12.6 | 1 |
| 243 | 0 | 1.8 | 0.4 | 5.3 | 0.8 | 13.6 | 14.4 | 1 | 0.9 | 1.6 | 0.4 | 4.6 | 0.9 | 10.4 | 11.3 | 1 |
| 244 | 0.7 | 1.4 | 1.1 | 3.8 | 2.4 | 8.1 | 10.5 | 1 | 1.2 | 1.1 | 1.2 | 4.3 | 1.2 | 8.9 | 10.1 | 1 |
| 247 | 0.5 | 0.9 | 0.6 | 3.4 | 3.6 | 7.4 | 11 | 1 | 0.5 | 2 | 0.6 | 3.8 | 2.5 | 8.1 | 10.6 | 1 |
| 248 | 1.1 | 1.6 | 1.6 | 4.3 | 3.7 | 8.9 | 12.6 | 2 | 2.1 | 1.8 | 0.9 | 2.3 | 2.1 | 8.6 | 10.7 | 1 |
| 250 | 0.6 | 0.7 | 0.7 | 3.3 | 2.1 | 6.7 | 8.8 | 1 | 1 | 1 | 0.4 | 2.6 | 1.2 | 6.3 | 7.5 | 1 |
| 252 | 1.4 | 1.8 | 0.4 | 7.2 | 1.1 | 12.4 | 13.5 | 1 | 2 | 1.7 | 0.5 | 5.8 | 1.4 | 11 | 12.4 | 1 |
| 257 | 0.8 | 1.3 | 0.9 | 4.8 | 0.9 | 12.8 | 13.7 | 1 | 0.3 | 1.5 | 0.6 | 4.5 | 0.9 | 11.9 | 12.8 | 1 |
| 265 | 0 | 1.4 | 0.7 | 3.8 | 1.5 | 8.2 | 9.7 | 1 | 0 | 1.7 | 0.5 | 3 | 1.4 | 7.2 | 8.6 | 1 |
| 270 | 0 | 1.5 | 0 | 7.4 | 0.4 | 13 | 13.4 | 1 | 0 | 1.3 | 0 | 4.2 | 0.6 | 11.8 | 12.4 | 1 |
| 277 | 1.1 | 0 | 0.5 | 3.3 | 1.9 | 6.4 | 8.3 | 1 | 0.7 | 1.8 | 0.8 | 4.3 | 1.3 | 6.5 | 7.8 | 1 |

Data of Arch type T : Taper arch form

| Case No. | 11_Li | 11_Pi | 11_Lm | 11_Pm | 11_La | 11_Pa | 11_LaPa | 11_SRP | 21_Li | 21_Pi | 21_Lm | 21_Pm | 21_La | 21_Pa | 21_LaPa | 21_SRP |
|---|---|---|---|---|---|---|---|---|---|---|---|---|---|---|---|---|
| 3 | 1.2 | 1.6 | 0.9 | 3.6 | 1.1 | 7.2 | 8.3 | 1 | 1.2 | 1.3 | 0.8 | 3.8 | 1.1 | 8 | 9.1 | 1 |
| 5 | 0.8 | 1 | 1 | 2.8 | 0.9 | 7 | 7.9 | 1 | 0 | 1 | 0.8 | 3.2 | 0.6 | 7.1 | 7.7 | 1 |
| 6 | 1.2 | 1.2 | 1.4 | 1.7 | 3.7 | 3.4 | 7.1 | 2 | 1.2 | 1.2 | 1.4 | 1.7 | 3 | 3.7 | 6.7 | 2 |
| 21 | 0.9 | 1.7 | 0.7 | 4.5 | 2.1 | 7 | 9.1 | 1 | 1 | 1.4 | 0.6 | 4.6 | 2.1 | 7 | 9.1 | 1 |
| 29 | 0.7 | 1.1 | 0.9 | 3.3 | 1.1 | 8.3 | 9.4 | 1 | 0 | 1.9 | 1.5 | 4.4 | 1.9 | 8.6 | 10.5 | 1 |
| 35 | 1.6 | 0.6 | 1.5 | 2 | 2.8 | 8.9 | 11.7 | 1 | 1.2 | 0.9 | 1.3 | 2 | 2.8 | 8.1 | 10.9 | 1 |
| 51 | 0.8 | 0.5 | 1 | 3.7 | 2.2 | 11.7 | 13.9 | 1 | 0.8 | 0.5 | 0.8 | 5.5 | 1.9 | 11.6 | 13.5 | 1 |
| 59 | 1.1 | 1.4 | 1.5 | 7 | 2.7 | 13 | 15.7 | 1 | 0.9 | 1.5 | 1 | 7.9 | 1.9 | 12.2 | 14.1 | 1 |
| 69 | 1.2 | 1.5 | 1.8 | 4 | 2.3 | 8.3 | 10.6 | 1 | 0.7 | 1.7 | 1.1 | 4.8 | 1.8 | 8.8 | 10.6 | 1 |
| 70 | 0.6 | 2.2 | 0.6 | 5.9 | 0.7 | 9.9 | 10.6 | 1 | 0.7 | 1.3 | 0.7 | 4.6 | 1.4 | 8.5 | 9.9 | 1 |
| 78 | 1 | 1.7 | 1.3 | 4.9 | 2.3 | 9.9 | 12.2 | 1 | 0.9 | 1.7 | 0.7 | 3.1 | 2.2 | 8.9 | 11.1 | 1 |
| 79 | 1.4 | 0.7 | 1.3 | 2.6 | 1.5 | 7.6 | 9.1 | 1 | 0.7 | 0.8 | 1.1 | 2 | 1.8 | 6.5 | 8.3 | 1 |
| 84 | 0.5 | 1.9 | 0.4 | 4.5 | 0.9 | 10.5 | 11.4 | 1 | 0.9 | 2.4 | 0.4 | 5.1 | 0.8 | 9.9 | 10.7 | 1 |
| 97 | 0.4 | 1.2 | 0.9 | 3 | 2.8 | 6.8 | 9.6 | 1 | 0.7 | 1.2 | 0.9 | 3.1 | 2.5 | 7.6 | 10.1 | 1 |
| 101 | 0.5 | 1.4 | 0.9 | 4.1 | 0.9 | 11.9 | 12.8 | 1 | 0.9 | 2.2 | 0.9 | 5.2 | 0.9 | 10.3 | 11.2 | 1 |
| 102 | 1.3 | 2.1 | 0.8 | 4 | 1.3 | 8.6 | 9.9 | 1 | 1.6 | 1.8 | 0.6 | 5.6 | 1 | 11.3 | 12.3 | 1 |
| 106 | 1.3 | 1.8 | 0.7 | 3.9 | 1.5 | 8.2 | 9.7 | 1 | 1.2 | 2 | 0.7 | 3.2 | 1.7 | 8.1 | 9.8 | 1 |
| 114 | 0.5 | 1.3 | 0.5 | 2.3 | 1.7 | 5.9 | 7.6 | 1 | 0.5 | 0.7 | 0.5 | 1.4 | 1.7 | 5 | 6.7 | 1 |

Data of Arch type T : Taper arch form

| Case No. | 11_Li | 11_Pi | 11_Lm | 11_Pm | 11_La | 11_Pa | 11_LaPa | 11_SRP | 21_Li | 21_Pi | 21_Lm | 21_Pm | 21_La | 21_Pa | 21_LaPa | 21_SRP |
|---|---|---|---|---|---|---|---|---|---|---|---|---|---|---|---|---|
| 123 | 1.1 | 0.9 | 0.8 | 6.6 | 2.5 | 12.6 | 15.1 | 1 | 0.9 | 1.9 | 0.6 | 5.4 | 0.9 | 11.4 | 12.3 | 1 |
| 128 | 1.1 | 1 | 0.7 | 0.9 | 1.5 | 5.3 | 6.8 | 1 | 1.6 | 1.4 | 0.7 | 2.6 | 0.9 | 6.4 | 7.3 | 1 |
| 131 | 1.5 | 0 | 1.3 | 4.9 | 2 | 10 | 12 | 1 | 1.2 | 1.2 | 1.3 | 4.8 | 2.3 | 8.8 | 11.1 | 1 |
| 140 | 1.4 | 1.7 | 0.9 | 4.1 | 2 | 8.3 | 10.3 | 1 | 1.1 | 1.7 | 1.1 | 3.2 | 1.6 | 6.5 | 8.1 | 1 |
| 146 | 0.4 | 1.5 | 0.4 | 3.2 | 2.6 | 6.1 | 8.7 | 1 | 0.7 | 1.5 | 0.6 | 3.7 | 2.6 | 6.5 | 9.1 | 1 |
| 153 | 0.3 | 1.7 | 0.5 | 3.8 | 1.2 | 5.8 | 7 | 1 | 0.3 | 1.2 | 0.6 | 3 | 1.3 | 6.4 | 7.7 | 1 |
| 157 | 0.7 | 1.5 | 1.3 | 2.3 | 1.7 | 5.1 | 6.8 | 1 | 0.7 | 2.1 | 1 | 3 | 1.5 | 5.9 | 7.4 | 1 |
| 161 | 0 | 0 | 0.9 | 2.9 | 1.6 | 9.4 | 11 | 1 | 1 | 0.7 | 0.9 | 4.4 | 1.6 | 9.5 | 11.1 | 1 |
| 165 | 0.7 | 1.1 | 0.5 | 2.5 | 0.7 | 8.9 | 9.6 | 1 | 0.5 | 0.9 | 0.5 | 2.6 | 1 | 10 | 11 | 1 |
| 166 | 0.8 | 1.1 | 1.2 | 4.4 | 2.4 | 6.2 | 8.6 | 1 | 1.1 | 0.8 | 1.4 | 2.3 | 0.8 | 6.4 | 7.2 | 1 |
| 174 | 0.6 | 1.3 | 0.6 | 4.2 | 0.9 | 8.9 | 9.8 | 1 | 0.5 | 1 | 0.6 | 4.4 | 0.9 | 7.9 | 8.8 | 1 |
| 177 | 1.3 | 3.5 | 0.5 | 6 | 2.1 | 11.8 | 13.9 | 1 | 0.7 | 2.3 | 0.5 | 5.7 | 2.1 | 10.5 | 12.6 | 1 |
| 179 | 0.4 | 1.9 | 0.5 | 3.1 | 2 | 5.9 | 7.9 | 1 | 0.6 | 2.2 | 0.7 | 3.4 | 2.1 | 7.7 | 9.8 | 1 |
| 180 | 0.5 | 1.1 | 1 | 2.6 | 1.9 | 11.6 | 13.5 | 1 | 0.8 | 3.1 | 1.1 | 6.2 | 1.9 | 12.7 | 14.6 | 1 |
| 181 | 1.3 | 1.3 | 1 | 2 | 1.4 | 7.5 | 8.9 | 1 | 1.2 | 0.9 | 0.9 | 2.8 | 1.4 | 7.6 | 9 | 1 |
| 184 | 0.7 | 3 | 1.7 | 5.1 | 3.4 | 11.5 | 14.9 | 1 | 0.5 | 1.1 | 0.9 | 4.6 | 2.4 | 9.9 | 12.3 | 1 |
| 190 | 0.6 | 1.2 | 0.5 | 2 | 2.7 | 6.4 | 9.1 | 1 | 0.8 | 0.6 | 1 | 1 | 1.8 | 3.7 | 5.5 | 1 |
| 192 | 0 | 0.9 | 0.5 | 1.6 | 1.7 | 5.4 | 7.1 | 1 | 0 | 1.1 | 0.7 | 2.1 | 1.3 | 4.7 | 6 | 1 |

Data of Arch type T : Taper arch form

| Case No. | 11_Li | 11_Pi | 11_Lm | 11_Pm | 11_La | 11_Pa | 11_LaPa | 11_SRP | 21_Li | 21_Pi | 21_Lm | 21_Pm | 21_La | 21_Pa | 21_LaPa | 21_SRP |
|---|---|---|---|---|---|---|---|---|---|---|---|---|---|---|---|---|
| 212 | 1.7 | 1.1 | 1.3 | 3.8 | 1.9 | 7.4 | 9.3 | 1 | 1.7 | 0.8 | 1.1 | 3.6 | 1.1 | 6.5 | 7.6 | 1 |
| 213 | 1 | 1.6 | 0.7 | 2.8 | 1.8 | 7 | 8.8 | 1 | 1 | 0.8 | 1 | 2.3 | 1.8 | 7.7 | 9.5 | 1 |
| 215 | 0.7 | 1.5 | 0.9 | 3.3 | 3.7 | 5.4 | 9.1 | 1 | 0.9 | 2.8 | 0.7 | 4.8 | 3.7 | 7.2 | 10.9 | 1 |
| 217 | 0.5 | 2.2 | 1.3 | 4.5 | 0.8 | 12.7 | 13.5 | 1 | 1 | 1.8 | 1.1 | 4.3 | 0.8 | 10.7 | 11.5 | 1 |
| 219 | 1.5 | 0 | 1.2 | 3 | 2.8 | 5.5 | 8.3 | 1 | 1.2 | 0 | 1.4 | 3 | 2.8 | 6.1 | 8.9 | 1 |
| 220 | 1.2 | 2.7 | 1 | 7.6 | 1.9 | 12.8 | 14.7 | 1 | 1 | 2.5 | 1.1 | 6.5 | 2.2 | 11 | 13.2 | 1 |
| 225 | 1.3 | 1.6 | 1 | 3.3 | 1 | 8.2 | 9.2 | 1 | 1.1 | 1.6 | 1.1 | 3.1 | 2.1 | 6.1 | 8.2 | 1 |
| 228 | 1.1 | 0.7 | 0.7 | 2.2 | 1.3 | 6.3 | 7.6 | 1 | 1.3 | 1.7 | 0.7 | 3.6 | 1.3 | 7.2 | 8.5 | 1 |
| 231 | 1.4 | 1.3 | 1.2 | 5.7 | 2.6 | 10.2 | 12.8 | 1 | 2.2 | 1.8 | 0.7 | 6.8 | 1.1 | 10.9 | 12 | 1 |
| 234 | 1.1 | 1.1 | 0.5 | 4.8 | 2.2 | 8.2 | 10.4 | 1 | 0.4 | 0.7 | 0.4 | 4.9 | 1.7 | 9.2 | 10.9 | 1 |
| 238 | 1.8 | 1.3 | 1.8 | 2.9 | 2.3 | 8.5 | 10.8 | 1 | 1.4 | 0.5 | 0.9 | 3.8 | 1.4 | 7.2 | 8.6 | 1 |
| 242 | 0 | 1.2 | 0.9 | 2.6 | 2.3 | 6.1 | 8.4 | 1 | 0 | 1.2 | 1.2 | 3.3 | 2.1 | 6 | 8.1 | 1 |
| 245 | 1.5 | 1 | 0.6 | 3.4 | 2.1 | 7.5 | 9.6 | 1 | 0.6 | 0.8 | 0.9 | 1.8 | 3.5 | 5.1 | 8.6 | 1 |
| 249 | 1.2 | 0.5 | 1.5 | 2.3 | 2.7 | 5.8 | 8.5 | 1 | 1.3 | 1.9 | 0.7 | 3.6 | 2.2 | 7.1 | 9.3 | 1 |
| 251 | 0.6 | 1 | 0.9 | 3.4 | 2.6 | 8.5 | 11.1 | 1 | 0.7 | 0.9 | 0.7 | 4.2 | 2.6 | 8.3 | 10.9 | 1 |
| 254 | 1.2 | 0.6 | 1.1 | 1.5 | 3.6 | 6.8 | 10.4 | 1 | 1.2 | 0.8 | 1 | 1.9 | 2.4 | 6.3 | 8.7 | 1 |
| 255 | 0.7 | 1.2 | 2.2 | 3 | 5.6 | 6.9 | 12.5 | 2 | 1.2 | 1.2 | 1.9 | 3.8 | 4.7 | 7 | 11.7 | 2 |
| 259 | 0.8 | 1.6 | 1 | 4.1 | 2.2 | 8.2 | 10.4 | 1 | 0 | 2 | 0.7 | 3.9 | 2.3 | 7.5 | 9.8 | 1 |

Data of Arch type T : Taper arch form

| Case No. | 11_Li | 11_Pi | 11_Lm | 11_Pm | 11_La | 11_Pa | 11_LaPa | 11_SRP | 21_Li | 21_Pi | 21_Lm | 21_Pm | 21_La | 21_Pa | 21_LaPa | 21_SRP |
|---|---|---|---|---|---|---|---|---|---|---|---|---|---|---|---|---|
| 271 | 0 | 0.9 | 0.5 | 3.1 | 1.7 | 6.7 | 8.4 | 1 | 0 | 0 | 0.8 | 2.2 | 2.5 | 6.2 | 8.7 | 1 |
| 272 | 0.6 | 1 | 0.7 | 2 | 0.9 | 7.2 | 8.1 | 1 | 0.4 | 0.6 | 0.5 | 4.2 | 1.3 | 9.1 | 10.4 | 1 |
| 274 | 0.6 | 2.5 | 1.2 | 7.5 | 3.3 | 12.2 | 15.5 | 1 | 1.1 | 1.5 | 0.8 | 5.1 | 2.4 | 9.5 | 11.9 | 1 |
| 275 | 2.2 | 2.2 | 1.2 | 5 | 2.1 | 9.3 | 11.4 | 1 | 1.7 | 2.2 | 1.2 | 5.1 | 2.2 | 9.2 | 11.4 | 1 |
| 276 | 0 | 1.5 | 0.5 | 2.4 | 2 | 6.2 | 8.2 | 1 | 0.5 | 1.8 | 0.5 | 3.2 | 1.1 | 7.6 | 8.7 | 1 |

# VITA

| | |
|---|---|
| **NAME** | สุทธิเกียรติ สมวสุนธรา |
| **DATE OF BIRTH** | 09 กุมภาพันธ์ 2532 |
| **PLACE OF BIRTH** | กรุงเทพมหานคร |
| **INSTITUTIONS ATTENDED** | ทันตแพทยศาสตร์บัณฑิต มหาวิทยาลัยรังสิต<br>Certificated of Advanced Implant Dentistry, UCLA |
| **HOME ADDRESS** | 76 ถ.กรุงเกษม แขวงบางขุนพรหม เขตพระนคร กรุงเทพมหานคร 10200 |
| **PUBLICATION** | - |
| **AWARD RECEIVED** | - |